ISSN 1070-3284, Russian Journal of Coordination Chemistry, 2022, Vol. 48, No. 11, pp. 675–695. © Pleiades Publishing, Ltd., 2022.
Russian Text © The Author(s), 2022, published in Koordinatsionnaya Khimiya, 2022, Vol. 48, No. 11, pp. 647–668.

Chelating Agents for Zirconium-89 in the Synthesis of Radiopharmaceuticals: Current State and Prospects of Development

V. B. Bubenshchikov[a], * and A. A. Larenkov[a]

[a] *Burnazyan Federal Medical Biophysical Center, Federal Medical and Biological Agency of Russia, Moscow, Russia*
**e-mail: bubenschikov2011@yandex.ru*

Received February 3, 2022; revised April 11, 2022; accepted April 14, 2022

Abstract—Zirconium is a highly demanded element widely used in various fields of science and technology. There are 39 known zirconium isotopes, among which zirconium-89 ($T_{1/2}$ = 78.42 h) attracts increasing attention of the scientific community in connection with the radionuclide diagnostics of various diseases. The radiopharmaceuticals based on ^{89}Zr are currently actively developed and introduced into clinical practice. The ^{89}Zr isotope is in demand to develop agents based on monoclonal antibodies, which are mainly used for cancer diagnosis and therapy monitoring. For incorporation of ^{89}Zr into vector molecules that would allow selective isotope accumulation in various foci, an appropriate chelating agent is required. Furthermore, specific features of application of zirconium-89 complexes in radiopharmaceuticals impose additional requirements on the chelator properties. First, this is high complex formation efficiency without heating of the reaction mixture at approximately neutral pH. Also, the complexes should be stable not only in vitro, but also in vivo. The main difficulty hampering the design of new chelators is the intricate coordination chemistry of zirconium, that is, the formation of polynuclear species with different degrees of polymerization and composition varying depending on pH and time. Therefore, conventional techniques such as EXAFS, X-ray diffraction, and potentiometric titration in aqueous media are often of low utility, and chemists have to resort to some alternative methods for studying these compounds. Thus, the integration of experimental data from various sources is of high practical value. The review discusses problems associated with the use of the popular chelator deferoxamine, recent advances in the search and synthesis of new chelators, and the application of various methods to evaluate the applicability of the obtained complexes for advanced nuclear medicine procedures.

Keywords: zirconium-89, chelators, deferoxamine, radiopharmaceuticals, positron emission tomography
DOI: 10.1134/S1070328422110021

INTRODUCTION

Positron emission computed tomography (PET) is a highly demanded method for molecular imaging used to diagnose various diseases. In recent years, imaging agents based on monoclonal antibodies (mAbs) have been actively developed and introduced into clinical practice. Combination of high selectivity of monoclonal antibodies and high sensitivity of PET promoted the development of a separate area of PET, immunoPET, directed towards cancer diagnosis and planning and monitoring of cancer therapy [1]. A distinctive feature of mAbs is slow pharmacokinetics of radiopharmaceuticals (RPs) based on them; as a result, the optimal biodistribution is usually reached not sooner than 24 h after the administration. On a set of nuclear and physical characteristics, the most appropriate PET radionuclides for the design of RPs based on mAbs are ^{124}I ($T_{1/2}$ = 4.17 days), ^{64}Cu ($T_{1/2}$ = 12.7 h), ^{86}Y ($T_{1/2}$ = 14.7 h), and ^{89}Zr ($T_{1/2}$ = 78.42 h). In this series, ^{89}Zr is favorably differs, as it has more suitable half-life than ^{64}Cu or ^{86}Y and forms more stable labeled species than ^{124}I both in vitro and in vivo [2, 3]. Zirconium-89 has almost ideal nuclear and physical characteristics for immunoPET. Owing to the long ^{89}Zr half-life ($T_{1/2}$ = 78.42 h), its biodistribution can be evaluated for up to 30 days after administration [4], and low energy of emitted positrons makes it possible to obtain high-resolution PET images [5–7].

Currently ^{89}Zr is used most widely to develop RPs based on labeled cells, monoclonal antibodies, and their fragments. The most recent achievements in this area related to clinical application of ^{89}Zr are covered in detail in recent reviews [8–12]. Zirconium-89 is usually introduced into vector molecules using bifunctional chelators that are capable of forming kinetically

inert and thermodynamically stable complexes with the radionuclide and a covalent bond with the vector molecule. However, when conducting the synthesis, one should bear in mind that many vectors (especially mAbs) cannot withstand the harsh reaction conditions normally required for complex formation (elevated temperature, non-neutral pH). This review is devoted to the development and evaluation of various promising ^{89}Zr chelators for further advancement of the diagnostic potential of immunoPET.

NUCLEAR AND PHYSICAL CHARACTERISTICS, PREPARATION, AND ISOLATION OF ZIRCONIUM-89

Zirconium-89 ($T_{1/2}$ = 78.42 h) decays via electron capture (77.2%) and positron emission (22.8%, $E_{\beta+}$ = 902 keV) to metastable ^{89m}Y ($T_{1/2}$ = 15.84 s), which decays to stable ^{89}Y (IT, $E\gamma$ = 909 keV, G_γ = 99.0%) (Scheme 1) [13].

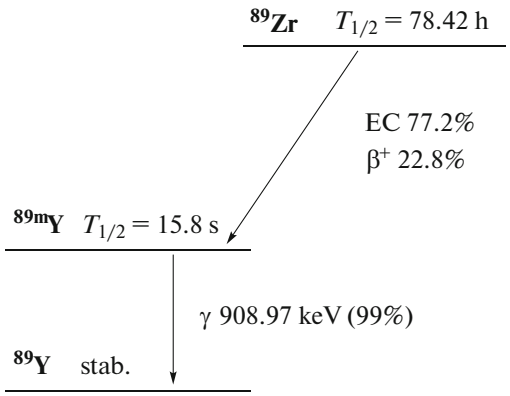

Scheme 1.

Currently, there are several ways for production of ^{89}Zr, proton irradiation of the yttrium target being the most popular one: ^{89}Y(p, n) ^{89}Zr. The key advantage of this method is the possibility of obtaining ^{89}Zr on low-energy cyclotrons by irradiation of a target made of monoisotopic natural yttrium [14–16]. A variety of methods were proposed to isolate ^{89}Zr from the irradiated target; the most popular one is the solid-phase extraction on hydroxamate-modified resins [15, 17, 18]. Using this method, ^{89}Zr is obtained as [^{89}Zr]Zr-oxalate in a high yield and with a high activity concentration [18, 19]. An alternative approach is to isolate ^{89}Zr as the [^{89}Zr]Zr-chloride [20, 21]. This method is less popular, since the [^{89}Zr]Zr-chloride is unstable at neutral pH and is mainly used for research purposes, while ^{89}Zr-mAb RPs are synthesized most often using [^{89}Zr]Zr-oxalate [22].

ZIRCONIUM COORDINATION CHEMISTRY

The chemistry of zirconium in aqueous solutions is complicated, due to the diversity of the possible chemical species. Zirconium has oxidation states of +2, +3, and +4 and forms complexes with different geometry and coordination numbers (C.N.) from 4 to 12 [23, 24]. The preferred oxidation state is +4 and preferred C.N. is 8. Some knowledge of zirconium chemistry is derived from hafnium chemistry, as these elements form compounds of similar properties. The similarity of compounds is related to the contraction of atomic (Hf = 1.44 Å and Zr = 1.45 Å) and ionic radii (Hf = 0.85 Å and Zr = 0.86 Å) on going from La to Lu and decrease in the Hf radius to become equal to the Zr radius [25]. Owing to the high charge density and small ionic radius, the Zr^{4+} cation is a hard Lewis acid; therefore, groups that behave as hard Lewis bases (i.e., those containing nitrogen and oxygen) are preferred for complex formation.

Initially, well-known chelators such as ethylenediaminetetraacetic acid (EDTA) and diethylenetriaminepentaacetic acid (DTPA) have been used to chelate Zr^{4+} (Scheme 2). Crystal structure studies of Zr-EDTA and Zr-DTPA demonstrated that Zr^{4+} forms eight-coordinate complexes in both cases and that Zr-EDTA additionally involves two water molecules [26, 27]. The authors did not consider the formation of polynuclear complexes. Despite relatively high thermodynamic stability constants ($\log\beta = 27.9 \pm 0.1$ for Zr(EDTA); $\log\beta = 35.3 \pm 0.3$ for Zr(DTPA) [28]), in practice, Zr(DTPA) proved to be insufficiently stable. Upon incubation in blood plasma for 24 h, the ^{88}Zr complex with DTPA partly dissociated (80% of the complex was retained), whereas the complex with deferoxamine (DFO) was stable (99.8% of the complex was retained) [29]. Deferoxamine was first isolated in 1960 from *Streptomyces pilosus* [30]. The hexadentate chelator DFO is a bifunctional siderophore containing three successively linked hydroxamate groups (Scheme 2). In view of Zr^{4+} proneness to react with hard Lewis bases and ability to form complexes with monohydroxamates, the authors of [29] showed

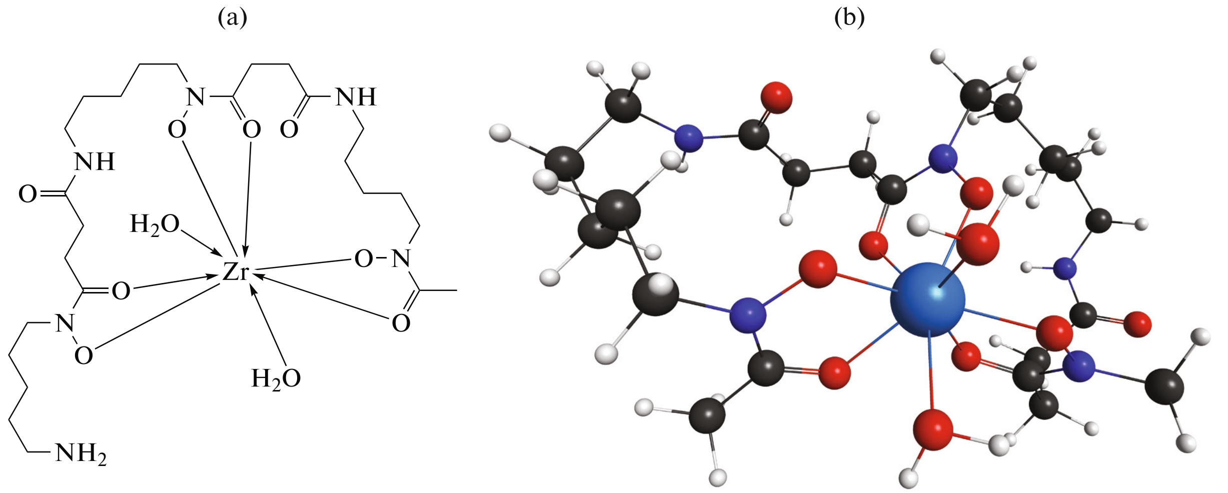

Fig. 1. (a) Simplified structural formula of the complex $[ZrDFO(H_2O)_2]^+$; (b) structure of $[ZrDFO(H_2O)_2]^+$ calculated by the density functional theory. Constructed using data of [32].

in 1992 that DFO forms stable complexes with ^{89}Zr and can be used as a chelator for the synthesis of radio-immunoconjugates. The structures of DTPA, EDTA, and DFO are depicted in Scheme 2.

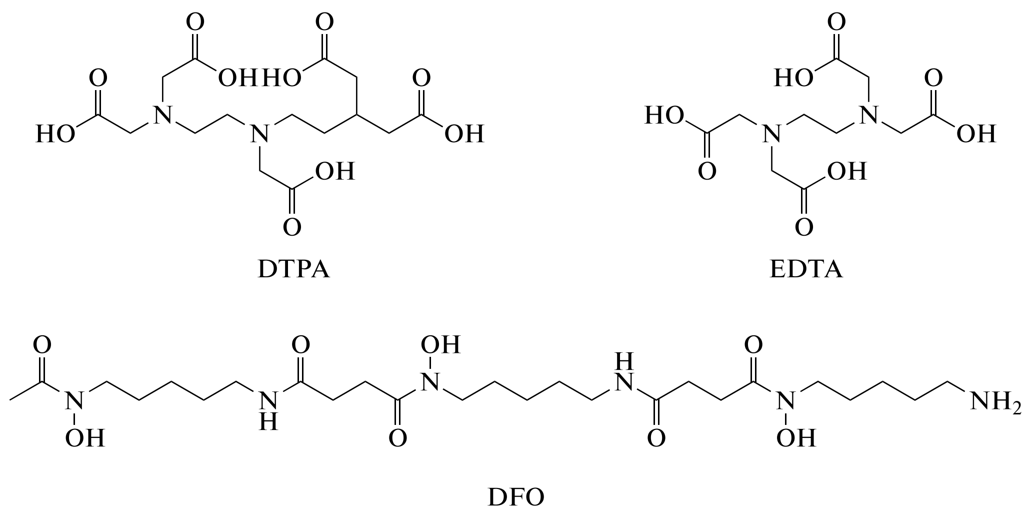

Scheme 2.

According to quantum chemical calculations, high stability of the $[^{89}Zr]$Zr-DFO complex is caused by $^{89}Zr^{4+}$ chelation by three hydroxamate groups of the DFO molecule. The complex is formed via three neutral and three negatively charged oxygen atoms, which coordinate the zirconium ion together with two water molecules (Fig. 1) [31]. The subsequent theoretical studies showed that Zr complexation with DFO in water gives $[Zr(DFO)(H_2O)_n]^+$ complexes (n = 0–2), among which $[ZrDFO(H_2O)]^+$ with C.N. = 7 is the most stable (logβ = 41.51) [32]. At the same time, the formation of $[ZrDFO(H_2O)]^+$ was confirmed experimentally [33]. Later, the authors of one more study (quantum chemical calculations, approximation of EXAFS results) came to the conclusion that the coordination sphere of Zr-DFO is, most likely, completed by two hydroxide ions rather than by two water molecules [34]. Thus, despite active studies, the exact structure of the Zr-DFO complex still remains unclear.

Determination of the exact structure and stability constants of Zr complexes in aqueous solutions is markedly complicated by the formation of poorly soluble polynuclear compounds with different degrees of polymerization and composition varying depending on the pH and time [35]. The accurate interpretation

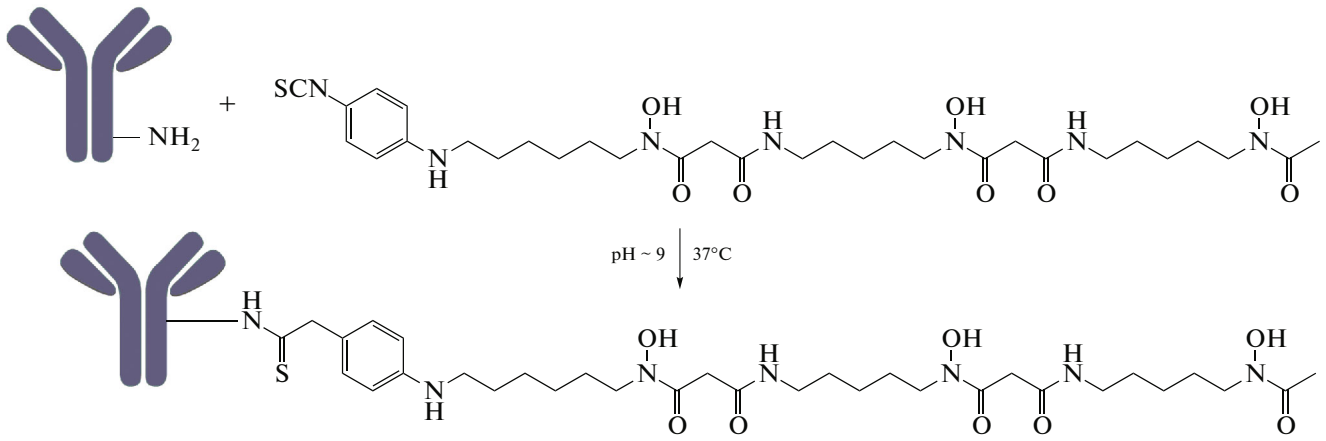

Fig. 2. Conjugation of mAb with p-Bn-NCS-DFO.

of the results and determination of adequate structural characteristics of zirconium complexes is also hampered by the fact that the data obtained using stable zirconium in analytical amounts cannot be extrapolated to systems in which zirconium is present as a trace component (no carrier added $^{89}Zr^{4+}$). Recently, several research groups published the results of determination of thermodynamic stability constants of the Zr-DFO complex [36–38]. The highest constant ($\log\beta = 49.1$) was found for $[Zr(HDFO)]^{2+}$, which was found to be the predominant species in the radiolabeling reaction (C_{DFO} = 1 μmol/L, pH 7) [38]. In [36], the constants $\log\beta = 46.4–47.7$ and 40.4 were reported for $[Zr(HDFO)]^{2+}$ and $Zr(DFO)]^{+}$, respectively; the deprotonated complex starts to predominate at pH ~ 6.4 ($C_{Zr(IV)} = 1$ mM, $C_{DFO} = 1$ mM). The lowest stability constants for $[Zr(DFO)]^{+}$ ($\log\beta$ = 36.14) were obtained in [37]. The authors noted that the stoichiometry of $[Zr(DFO)]^{+}$ complexes considerably varies as a function of the pH; when the zirconium and DFO concentrations are 1 mM, binuclear complexes with 2 : 2 and 2 : 3 Zr : DFO molar ratio are predominant species in solutions. The presence of these species in the systems with a picomolar content of zirconium (as is the case for no carrier added zirconium-89 radionuclide) is improbable.

It is noteworthy that for the choice of chelators for RPs, the kinetic stability is more important than the thermodynamic stability of the metal–chelate complex. The thermodynamic stability constants may be useful for preliminary comparison of various chelators, but do not reflect the stability of complexes in vivo. Meanwhile, the in vivo stability is the main criterion for the use of complexes in nuclear medicine [39]. When RPs are administered into the body, the target complex experiences some adverse impacts. The metal ions present in the body exist in much higher concentrations and can displace zirconium as a trace component from the complex. The situation is further complicated by the presence of strong native metal-binding transport proteins able to transchelate radionuclides [39]. For example, it was shown that Zr binds to transferrin, albumin fraction, and α-, β-, and γ-globulins [40, 41]. On the one hand, these factors force researchers to use indirect methods for determining the properties of zirconium-89 complexes, but, on the other hand, they provide a more practically significant evaluation of applicability of these compounds directly in vitro and in vivo.

Currently, deferoxamine is the gold-standard chelator for the synthesis of [^{89}Zr]Zr-mAb radiopharmaceuticals, owing to its ability to form stable complexes with many metals (including Zr) and commercial availability. A variety of methods have been proposed for linking DFO to mAb; the main drawback of the proposed protocols is still the large number of synthetic steps. These methods are considered in detail in a number of reviews [8, 42, 43]. A more facile, one-step method has been proposed for conjugation of p-Bn-NSC-DFO with the lysine amino group of non-modified antibody (Fig. 2) [44, 45]. The conjugation reaction is based on the formation of a thiourea bond and proceeds under mild conditions (37°C, 30 min). Sodium carbonate with pH 9 is used, most often, as the buffer.

However, hexadentate DFO is not the optimal Zr chelator, since Zr preferably forms complexes with C.N. = 8. This inconsistency is especially obvious when considering the biodistribution of [^{89}Zr]Zr-DFO-based agents. Some publications note high accumulation of ^{89}Zr (~10% of the injected dose per gram (%ID/g)) in the mouse skeleton after intravenous injection (i/v) of ^{89}Zr-DFO-mAb [31, 46–49]. The most plausible explanation to this fact is the release of zirconium-89 from the DFO complex. The high osteotropism of ^{89}Zr results in its uptake in bone tissue, which distorts the real biodistribution of the agent and may lead to false positive or false negative

results or underestimation of the radiation dose absorbed by the bone marrow [50, 51]. These results served as the starting point for the development of more advanced, mainly octadentate chelators for zirconium-89.

LINEAR HYDROXAMATES

The authors of [52] modified DFO by introducing an additional hydroxamate group and obtained chelators DFO* and DFOcyclo* (Scheme 3).

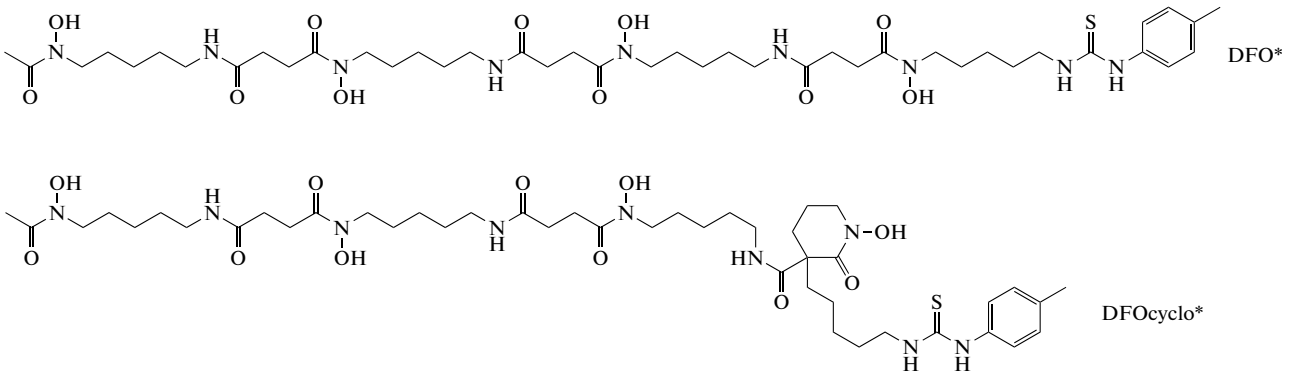

Scheme 3.

The octadentate chelator DFO* was conjugated with succinic anhydride to be subsequently used as a bifunctional chelating agent (BCA). Then the chelator was conjugated with bombesin and labeled with ^{89}Zr. To evaluate the stability, [^{89}Zr]Zr-DFO*-bombesin was incubated in an excess of DFO (the [^{89}Zr]Zr-DFO-bombesin reference sample was incubated in an excess of DFO*). The DFO*-based agent was more stable against transchelation than the agent based on the DFO. Later this study was continued by other researchers [53]. DFO* was conjugated with 1,4-phenylene diisothiocyanate and then with mAbs (trastuzumab, rituximab, and cetuximab). An interesting feature of this study is the ^{89}Zr pre-labeling of p-Bn-NCS-DFO* and p-Bn-NCS-DFO. In this case, the subsequent conjugation of the complex with mAb was possible only for [^{89}Zr]Zr-p-Bn-DFO*. The authors attributed this fact to the participation of the isothiocyanate linker in the formation of the [^{89}Zr]Zr-DFO complex; as a result it became inaccessible for the subsequent conjugation with mAb. The stability of [^{89}Zr]Zr-DFO-trastuzumab (**I**) and [^{89}Zr]Zr-DFO*-trastuzumab (**II**) was evaluated in vitro in blood serum, isotonic NaCl solution, and a solution containing 20 mM histidine and 240 mM saccharose. According to experimental data, sample **I** showed a higher immunoreactivity and stability in all three solutions. The data on blood serum stability are summarized in Table 1. A comparative study in vivo showed similar biodistribution (24 h after the injection). The subsequent observation (72 h, 144 h) revealed gradual decrease in the bone uptake for compound **I** and increase for compound **II**. Generally, compound **I** showed lower non-specific uptake, mainly in bone tissue (Table 1).

In a similar study [54], DFO and DFO* were conjugated with human immunoglobulin-G (hIgG) and trastuzumab emtansine (T-DM1). According to earlier studies, the latter provides more accurate imaging of HER2+ breast cancer than usual trastuzumab [59]. According to in vitro stability evaluation, [^{89}Zr]Zr-DFO*-hIgG was stable in blood plasma and in 0.1 mM EDTA solution for 5 days. The incubation of [^{89}Zr]Zr-DFO*-hIgG in an excess of DFO resulted in a minor release of ^{89}Zr (11.0 ± 1.9% after 24 h and 26.0 ± 2.1% after 5 days). A comparative in vivo study (NOD/SCID mice with SKOV-3 human ovarian cancer xenografts) showed a lower non-specific uptake of [^{89}Zr]Zr-DFO*-T-DM1 in all tissues (Table 1). It is noteworthy that a similar study on healthy BALB/c mice showed a much higher non-specific uptake in all tissues and organs: the blood uptake of [^{89}Zr]Zr-DFO*-T-DM1 within 96 h after injection was 8.4 ± 0.7%ID/g, whereas for NOD/SCID mice it was 0.1 ± 0.0%ID/g. The authors attributed this difference to lower IgG level in NOD/SCID mice, which led to higher mAb clearance from blood. In general, the results were in good agreement with previously published data [52, 53].

One more comparative study with DFO* was carried out in [55]. Apart from comparing DFO with DFO*, the authors synthesized a new octadentate chelator, DFOcyclo*-pPhe-NCS (Scheme 3). The conditions of synthesis of ^{89}Zr complexes for all of the considered chelators and the partition coefficients in the *n*-octanol–water system are summarized in Table 2. The ^{89}Zr complexes with DFO, DFO*, and DFOcyclo* were evaluated in blood plasma, a 1000-fold excess of EDTA and DFO. The authors noted the high stability of all complexes in blood plasma for 7 days (>98%). The highest stability in excess EDTA

Table 1. Results of *in vitro* and *in vivo* studies for linear hydroxamates

Chelator	Vector	Stability in vitro		Stability in vivo		Ref.
		method	intact complex, %	bone uptake, % of the injected dose per gram (%ID/g)	time point	
DFO	Trastuzumab	Blood serum (7 days)	72.0	3.9 ± 0.8	144 h	[53]
DFO*			96.3	0.8 ± 0.1		
DFO	T-DM1			9.6 ± 0.4	96 h	[54]
DFO*				6.6 ± 0.6		
DFO	Trastuzumab	1000-fold excess of EDTA (7 days)	~50%	4.5 ± 0.6	168 h	[55]
DFO*			>98%	2.0 ± 0.3		
DFOcyclo*			>98%	1.5 ± 0.3		
DFO	Trastuzumab			7.1 ± 0.8	96 h	[56]
Orn3-hx				10.0 ± 1.5		
Orn4-hx				7.0 ± 2.2		
DFO	Trastuzumab	Blood plasma (3 days)	55	7.6 ± 0.4	72 h	[57]
C[1]			3	19.5 ± 3.6		
C[2]			16	18.3 ± 2.9		
DFO*	Trastuzumab	375-fold excess of EDTA (1 days)	>90	0.8 ± 0.3	144 h	[58]
DFOSq			82	8.2 ± 0.8		
DFO			68	4.6 ± 2.3		
DFO*Sq			>90	1.2 ± 0.4		
DFO	HPG		97	3.3 ± 0.4		
DFO*	HPG		>99	3.1 ± 0.7		

was found for [^{89}Zr]Zr-DFOcyclo* and [^{89}Zr]Zr-DFO* (>98%), whereas in the case of [^{89}Zr]Zr-DFO, only 53% of the complex was unchanged after 7 days of incubation. Similar results in the presence of excess EDTA were obtained for [^{89}Zr]Zr-DFOcyclo*-trastuzumab (**III**), [^{89}Zr]Zr-DFO*-trastuzumab (**IV**), and [^{89}Zr]Zr-DFO-trastuzumab (**V**). In the presence of excess DFO, the agent **III** was much more stable (50% of intact complex after 48 h) than **IV** (50% after 4 h) or **V** (<50% after 1 h). A comparative in vivo study showed approximately the same pharmacokinetics for compounds **III**–**V** and lower uptake in bone tissue for the agents based on DFO* and DFOcyclo* compared to DFO (Table 1). It is important that DFO* has a higher lyophilicity (log$P$ = −0.44 [60]) and, as a consequence, the synthesis of ^{89}Zr RPs based on mAbs requires the use of a higher DMSO concentration, which in turn can induce protein aggregation [53].

In order to solve this problem, DFO was modified by introducing ether bridges into the molecule [73]. Using bioorganic synthesis, the authors obtained a number of DFO analogues containing one (DFO-O_1), two (DFO-O_2), or three (DFO-O_3) ether oxygen atoms (Scheme 4). Measurements of the partition

Table 2. Labeling conditions of various chelators and log*P* values of the resulting complexes[1]

Chelator	Labeling conditions	Yield of complexation reaction, %	log*P* ^{89}Zr-L	Ref.
DFO*	RT, 15 min	100	−3.5	[55]
DFOcyclo*	RT, 15 min	100	−2.1	[55]
Orn3-hx	RT, 20 min	100		[56]
Orn4-hx	RT, 20 min	100		[56]
oxoDFO*	RT, 120 min	100	−1.5	[60]
4HMS	RT, 7 min	100		[61]
DFO	RT, 90 min	100	−3.0	[62]
TAFC	RT, 90 min	100	−2.0	[62]
FSC(succ-RGD)$_2$AA	RT, 90 min	100	−3.3	[63]
FSC(succ-RGD)$_3$	RT, 90 min	100	−3.5	[63]
L^1	RT, 5 min	100	−1.4	[64]
L^2	RT, 5 min	100	−2.3	[64]
L^3	RT, 5 min	100	−2.1	[64]
L^4	RT, 5 min	100	−3.4	[64]
CTH36	RT, 60 min	100		[65]
DFO-HOPO	RT, 60 min	100	−0.9	[66]
BPDET-LysH22,2-3-HOPO	RT, 15 min	100	−1.5	[67]
THPN	RT, 10 min	100	−3.1	[68]
IAM-1	95°C, 120 min	100	−3.0	[69]
IAM-2	50°C, 60 min	100	−1.5	[69]
TAM-1	RT, 15 min	100	−3.4	[70]
TAM-2	RT, 15 min	100	−3.4	[70]
DOTA	99°C, 120 min (90°C, 45 min*)	65 ± 9.6 (100**)	−3.8	[71]
DOTP	99°C, 120 min (90°C, 45 min*)	70 ± 10.6 (100**)	−3.9	[71]
DOTAM	99°C, 120 min (90°C, 45 min*)	9 ± 1.3 (100**)	−1.4	[71]
PTCA	37°C, 60 min	100	−3.1	[72]
NOTA	37°C, 60 min	100	−2.5	[72]
TRITA	99°C, 120 min	100	−3.1	[72]

[1] Labeling conditions and radiochemical yields for reactions using a starting solution of [^{89}Zr]Zr-chloride; RT is room temperature.

coefficients in the *n*-octanol–water system (log*P*) showed that DFO-O_3 was approximately 45 times more hydrophilic than the initial DFO. Subsequently, the authors synthesized and compared a number of octadentate chelators similar to DFO [74]. Among these chelators (Scheme 4), the compound containing an ether bridge proved to form the least stable Zr(IV) complex (in terms of decreasing stabil-

ity, the order of chelators was as follows: DFOB-PBH ≈ DFOB-PPH > DFOB-PPH^{N}O^{C}O ≫ DFO), whereas the introduction of an additional methylene group into the hydrocarbon chain did not affect the stability, but led to an increase in the complex formation rate.

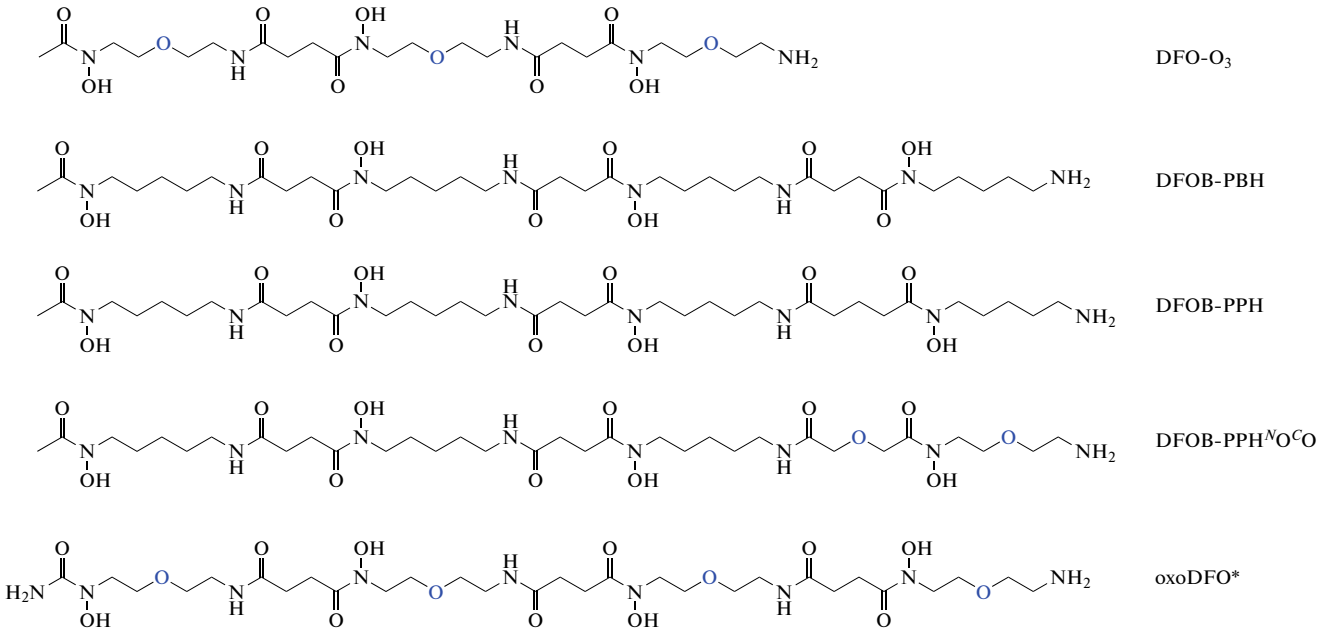

Scheme 4.

A similar approach was used in [60]. Using solid-phase synthesis, the authors obtained octadentate water-soluble DFO* derivative containing four ether bridges—oxoDFO* (Scheme 4, log$P$ = −1.5 ± 0.2). The stability of ^{89}Zr complexes with DFO, DFO*, and oxoDFO* was evaluated in a 5–50 mM excess of DTPA (pH 6). Under these conditions, the complexes [^{89}Zr]Zr-oxoDFO* ≥ [^{89}Zr]Zr-DFO* were more stable than [^{89}Zr]Zr-DFO [75]. In a similar study dealing with ^{68}Ga, a quantitative yield was attained only on heating and the obtained complexes were less stable in the presence of 5 mM DTPA ([^{68}Ga]Ga-DFO ≈ [^{68}Ga]Ga-DFO* > [^{68}Ga]Ga-oxoDFO*) than analogous ^{89}Zr complexes.

In an alternative study [56], the authors synthesized branched chelators Orn4-hx and Orn3-hx (Scheme 5), which were analogues of cyclic desferrichrome (DFC). The stability was measured in a 1000-fold excess of EDTA and was found to decrease in the series [^{89}Zr]Zr-Orn4-hx ~ [^{89}Zr]Zr-DFO > [^{89}Zr]Zr-DFC > [^{89}Zr]Zr-Orn3-hx, which is in good agreement with the results of quantum chemical calculations. Subsequently, these chelators were conjugated with 1,4-phenylene diisothiocyanate and then with trastuzumab and labeled with ^{89}Zr. A comparative in vivo assay on healthy mice showed identical bone tissue uptakes within 96 h after the injection for the [^{89}Zr]Zr-DFO-trastuzumab and [^{89}Zr]Zr-Orn4-hx-trastuzumab samples and a higher uptake for [^{89}Zr]Zr-Orn3-hx-trastuzumab (Table 1). Thus, the introduction of the additional fourth hydroxamate group into the chelator molecule (Orn3-hx → Orn4-hx) is necessary for the formation of stable complexes. Nevertheless, the ^{89}Zr complex with Orn4-hx was identical in the in vitro and in vivo stability to the complex with DFO.

The authors of one more study dealing with the synthesis of promising acyclic chelators [57] prepared two branched acyclic bifunctional chelators C^1 and C^2 based on tetrahydroxamate (Scheme 5). The obtained molecules as well as p-Bn-NCS-DFO were conjugated with trastuzumab and labeled with ^{89}Zr. The stability of the obtained agents was assessed in the mice blood plasma (incubation for 3 days at 37°C). The agents based on C^1 and C^2 proved to be less stable than [^{89}Zr]Zr-DFO-trastuzumab (Table 1). Comparative in vivo study showed a gradual increase in the ^{89}Zr uptake in bone tissue for all three agents. Three days after injection the bone tissue uptakes of [^{89}Zr]Zr-C^1-trastuzumab and [^{89}Zr]Zr-C^2-trastuzumab were considerably higher than that of [^{89}Zr]Zr-DFO-trastuzumab (Table 1). The unsatisfactory stability of C^1- and C^2-based agents was attributed to steric restrictions caused by the insufficient length of the hydrocarbon chains in the chelator backbone.

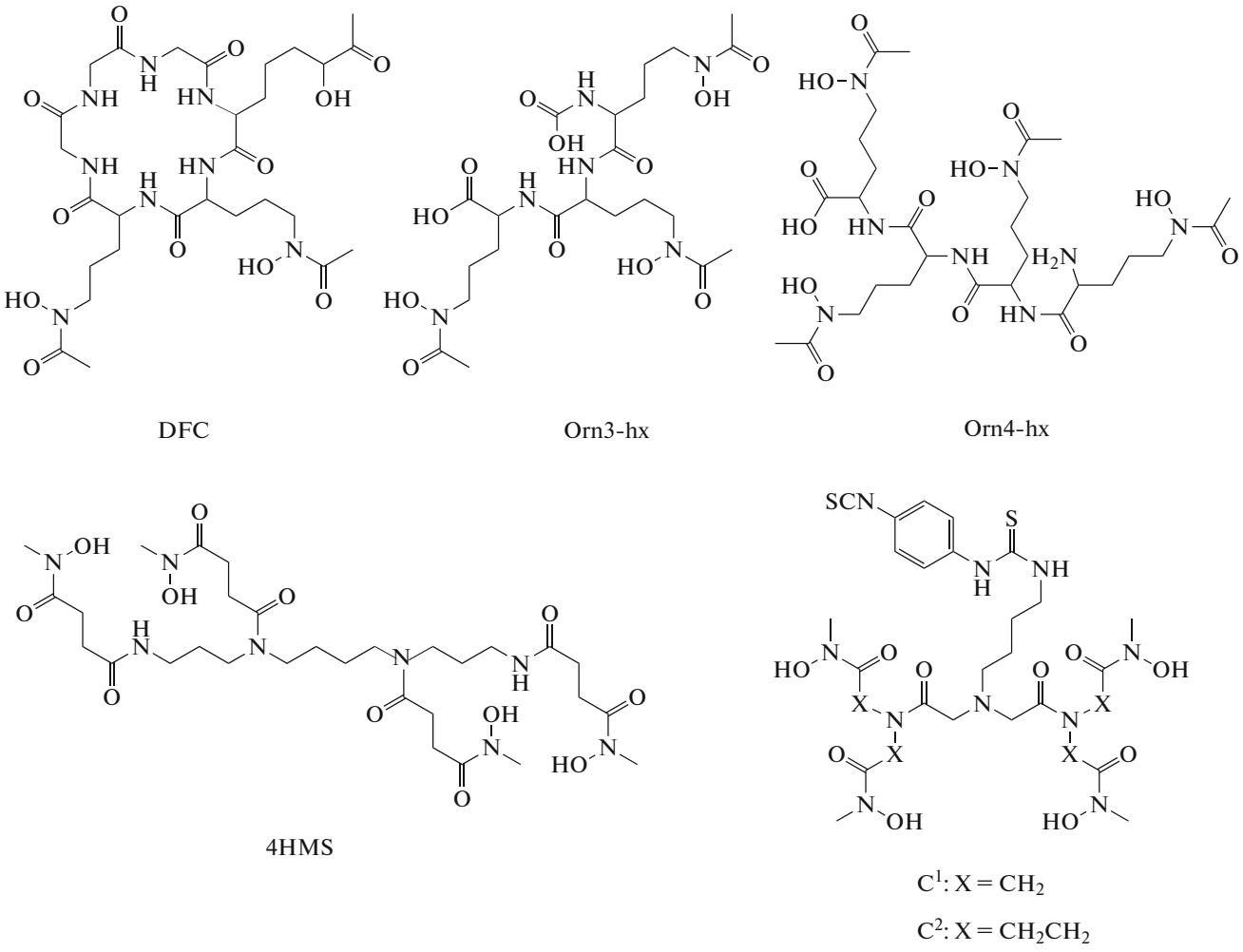

Scheme 5.

More successful results were obtained using the acyclic chelator 4HMS (Scheme 5) [61]. The formation of 1 : 1 complex of this ligand with zirconium was confirmed by mass spectrometry. The stability of the complex was assessed in an excess of DTPA (100- and 1000-fold excess, pH 5; 7; 8.5) in blood plasma and in the presence of excess metal salts (10-fold excess of Fe^{3+}, Co^{2+}, Cu^{2+}, Ni^{2+}, Mg^{2+}, and Ca^{2+}). In all test systems used, the [^{89}Zr]Zr-4HMS complex was stable (>97% of the complex was intact after 7 days) and was transchelated only in the presence of a 1000-fold excess of DTPA (91.9 ± 0.1% of the complex was intact after incubation for 7 days at 37°C) and a 100-fold excess of Fe^{3+} (62.3 ± 0.3% was intact after incubation for 7 days at 37°C). Under the same conditions, the [^{89}Zr]Zr-DFO complex was substantially transchelated (64.1 ± 0.8 and 33.8 ± 1.6% of the complex were intact, respectively). A comparative in vivo assay showed a faster excretion for [^{89}Zr]Zr-4HMS and low uptake in all organs and tissues, including bones (0.01 ± 0.0%ID/g 24 h after injection), compared with [^{89}Zr]Zr-DFO (bone uptake of 0.17 ± 0.13%ID/g 24 h after injection). Generally, the results attest to good prospects of 4HMS; however, additional experiments on the synthesis of bifunctional 4HMS derivative and determination of its long-term stability in vivo are required for further evaluation.

One more approach to modification of the DFO molecule was based on the synthesis of DFO-squaramide ester DFOSqOEt (Scheme 6) [76]. The main advantages of this chelator are easy synthetic procedure and higher water solubility in comparison with other modified DFO derivatives. The stability of DFOSqOEt in vivo was evaluated without preliminary in vitro assays. Two studies were carried out in which p-Bn-NCS-DFO and DFOSqOEt were conjugated with trastuzumab and chDAB4 (APOMAB®) [76, 77]. In both cases, the products synthesized using DFOSqOEt showed a lower liver and bone uptakes and higher tumor/background tissue, tumor/bone tissue, and tumor/liver differential uptake ratios (DURs) compared with p-Bn-NCS-DFO.

Table 3. Stability and immunoreactivity of compounds **VI**–**IX** in blood serum for 7 days [58]

Agent	Stability, %	Immunoreactivity, %
[^{89}Zr]Zr-DFO*-NCS-trastuzumab (**VI**)	94 ± 0	90 ± 1
[^{89}Zr]Zr-DFOSq-trastuzumab (**VII**)	87 ± 1	80 ± 1
[^{89}Zr]Zr-DFO-NCS-trastuzumab (**VIII**)	81 ± 1	74 ± 1
[^{89}Zr]Zr-DFO*Sq-trastuzumab (**IX**)	100 ± 0	96 ± 1

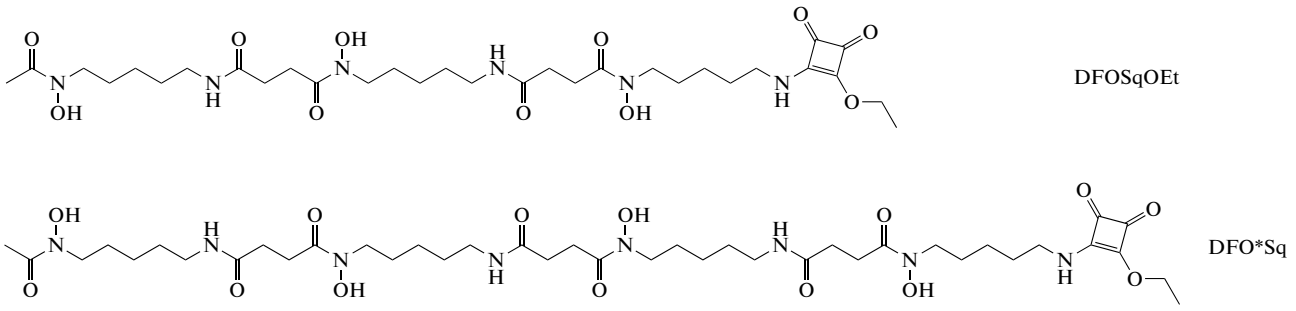

Scheme 6.

Later, a detailed comparison of the most promising modified DFO derivatives (DFO*-NCS, DFOSq) was reported [58]. The authors additionally synthesized the chelator DFO*Sq as a derivative of two different procedures. For comparative studies, these chelators were conjugated with trastuzumab. The stability of the resulting agents ([^{89}Zr]Zr-DFO*-NCS-trastuzumab (**VI**), [^{89}Zr]Zr-DFOSq-trastuzumab (**VII**), [^{89}Zr]Zr-DFO-NCS-trastuzumab (**VIII**), and [^{89}Zr]Zr-DFO*Sq-trastuzumab (**IX**)) was estimated in vitro in blood serum in the presence of a 375-fold excess of EDTA, DFO, and DFO*. The stability of the [^{89}Zr]Zr-DFO* and [^{89}Zr]Zr-DFO complexes was additionally evaluated in the presence of potentially competing metals (10-fold excess of Co^{2+}, Zn^{2+}, Cu^{2+}, Mg^{2+}, Ga^{3+}, Gd^{3+}, Al^{3+}, Fe^{3+}, and Nb^{3+}).

The incubation in blood serum (1 : 1) for 7 days at 37°C did not induce a considerable change in the radiochemical purity (RCP) for any of the agents (Table 3). In an excess of EDTA, complexes based on DFO* were more stable than DFO-based analogues (Table 1). The incubation in the presence of excess DFO was accompanied by a sharp decrease in RCP (less than 10% of the complex was retained) over 4 h for DFO-based agents (**VII** and **VIII**), whereas the agents based on **VI** and **IX** remained relatively stable for 24 h (>70%). The authors additionally noted high stability (>97%) of the [^{89}Zr]Zr-DFO* and [^{89}Zr]Zr-DFO complexes in the presence of Co^{2+}, Zn^{2+}, Cu^{2+}, Mg^{2+}, Ga^{2+}, Gd^{3+}, and Al^{3+}, minor substitution in the presence of Fe^{3+} (down to 93 ± 1% and 89 ± 2% for [^{89}Zr]Zr-DFO* and [^{89}Zr]Zr-DFO, respectively), and the sharp drop in the presence of Nb^{3+} (<10% was intact after 1 h of incubation for both complexes).

The prospects for application of the studied chelators in vivo were evaluated in a number of comparative studies of trastuzumab agents (**VI**–**IX**) on mice with. HER2+ antigen-expressing tumors; [^{89}Zr]Zr-DFO*-NCS-cetuximab and [^{89}Zr]Zr-DFO-NCS-cetuximab agents on mice with A431 tumor; and [^{89}Zr]Zr-DFO*-NCS-trastuzumab, [^{89}Zr]Zr-DFO-NCS-trastuzumab, [^{89}Zr]Zr-DFO*-NCS-B12, and [^{89}Zr]Zr-DFO-NCS-B12 agents (reference RPs with anti-HIV antibody) using a bone metastasis mouse model [58]. Generally, all results confirmed a higher stability of ^{89}Zr compounds based on DFO* complexes. In all three studies, DFO*-based agents (**VI** and **IX**) had a lower bone uptake than compounds **VII** and **VIII**. Despite higher in vitro stability, DFOSq-based samples (**VII** and **IX**) had a biodistribution similar to that characteristic of DFO-based samples (**VI** and **VIII**). The data for compounds **VI**–**IX** are summarized in Table 1. It is noteworthy that despite low solubility of p-Bn-NCS-DFO* and almost identical biodistribution profiles of the agents based on DFO* and DFO*Sq, the authors considered DFO*-NCS to be a more promising chelator due to higher rate of the conjugation reaction and commercial availability.

CYCLIC HYDROXAMATES

Complexation reactions and stability of ^{89}Zr complexes were studied for various hydroxamate-modified rings such as L [64, 78], CTH36 [65], fusarinine C (FSC), and its triacetylated analogue (TAFC) [62].

FSC is a macrocyclic chelator containing three hydroxamate groups and three primary amine groups, which can serve for bioconjugation. TAFC is the triacetylated analogue of FSC (Scheme 7) [62]. The

authors prepared a series of compounds based on the RGD peptide using various linkers: $FSC(RGDfE)_3$, $FSC(succ\text{-}RGD)_3$, and FSC(Mal-RGD). A comparative in vitro study of [^{89}Zr]Zr-TAFC, [^{89}Zr]Zr-$FSC(succ\text{-}RGD)_3$, and [^{89}Zr]Zr-DFO (incubation in excess EDTA for 7 days) revealed higher stability for [^{89}Zr]Zr-TAFC (97.2 ± 0.2% of the complex as intact) and [^{89}Zr]Zr-$FSC(succ\text{-}RGD)_3$ (93.9 ± 0.7%) than for [^{89}Zr]Zr-DFO (42.2 ± 2.3%). The incubation of [^{89}Zr]Zr-DFO in excess TAFC resulted in quantitative transchelation as soon as 1 h after mixing, whereas in the opposite case (incubation of [^{89}Zr]Zr-TAFC in excess DFO), the [^{89}Zr]Zr-TAFC complex was relatively stable (74.2 and 39.8% intact after 24 h and 7 days, respectively). An in vivo study of [^{89}Zr]Zr-$FSC(succ\text{-}RGD)_3$ showed high clearance from blood, low bone uptake, and predominant renal excretion 6 h after the injection. Similar results were obtained in vivo for [^{89}Zr]Zr-TAFC; however, note that no comparative studies with [^{89}Zr]Zr-DFO or [^{89}Zr]Zr-DFO-RGD in vivo were carried out.

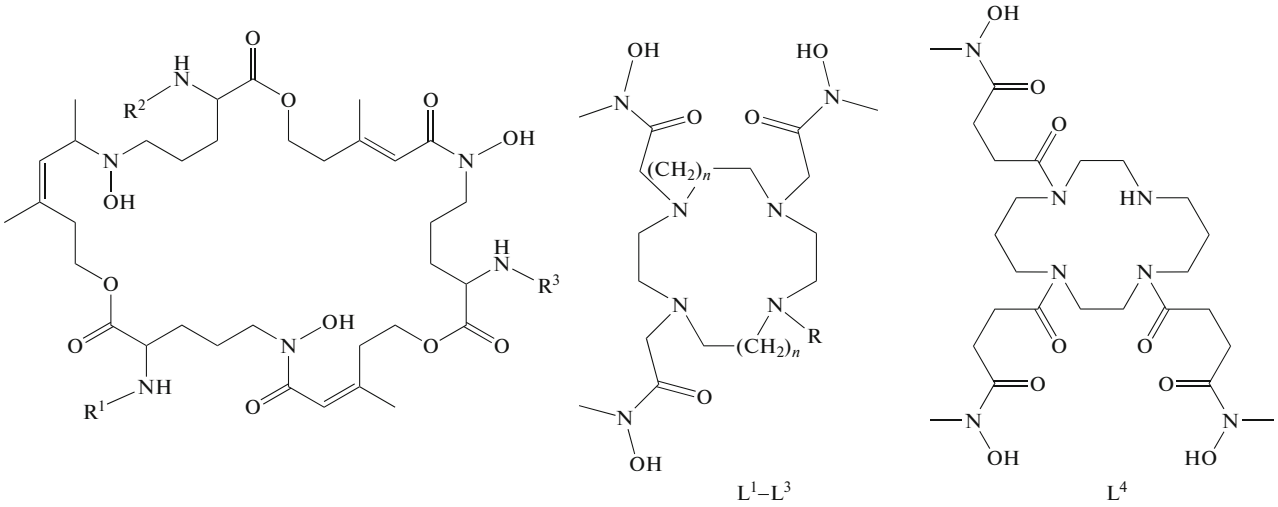

FSC: R^1; R^2; R^3 = H

TAFC: R^1; R^2; $R^3 = COCH_3$

$FSC(succ)_2$: R^1; $R^2 = COCH_2CH_2COOH$; R^3 = H

$FSC(succ)_2AA$: R^1; $R^2 = COCH_2CH_2COOH$; $R^3 = COCH_3$

$FSC(succ)_3$: R^1; R^2; $R^3 = COCH_2CH_2COOH$

L^1: n = 1, R = $CH_2CONOHCH_3$

L^2: n = 2, R = H

L^3: n = 2, R = $CH_2CONOHCH_3$

Scheme 7.

Subsequently, the authors conjugated FSC with succinic and acetic anhydrides to introduce additional coordination groups [63]. This gave the chelators $FSC(succ)_2$, $FSC(succ)_2AA$, and $FSC(succ)_3$ containing two or three additional succinate groups (Scheme 7). According to in vitro studies, all ^{89}Zr complexes were more stable than a similar complex with DFO. In terms of decreasing stability, the complexes can be arranged in the series [^{89}Zr]Zr-$FSC(succ)_3$ > [^{89}Zr]Zr-TAFC > [^{89}Zr]Zr-$FSC(succ)_2AA$ ≫ [^{89}Zr]Zr-DFO. A comparative in vivo study of [^{89}Zr]Zr-$FSC(succ)_3$ and [^{89}Zr]Zr-TAFC showed a slower clearance from blood for [^{89}Zr]Zr-$FSC(succ)_3$, together with a higher non-specific uptake in all major organs except for liver, intestines, and spleen, in which a higher uptake was found for [^{89}Zr]Zr-TAFC due to hepatobiliary excretion.

A direct comparison of FSC and DFO was performed in [79]. As the vector, the authors used an antibody fragment specific to epidermal growth factor receptors (ZEGFR:2377). The stability of [^{89}Zr]Zr-FSC-ZEGFR:2377 (**X**) and [^{89}Zr]Zr-DFO-ZEGFR:2377 (**XI**) was studied in PBS and in a 1000-fold excess of EDTA. The FSC-based sample was more stable in both media than the DFO-based one (stability data in EDTA are given in Table 4, which is in good agreement with the previously reported data on the comparison of [^{89}Zr]Zr-FSC and [^{89}Zr]Zr-DFO [63]).

The authors additionally noted that conducting the labeling reaction at 85°C leads to a slight increase in the stability of both complexes in vitro and in vivo. A comparative in vivo assay showed a lower clearance from blood, comparable bone uptake (Table 4), and higher uptake in all main organs and in the tumor for agent **X** (24 h after the injection, the tumor/blood

Table 4. Results of *in vitro* and *in vivo* studies for cyclic hydroxamates and chelators based on hydroxypyridone

Chelator	Vector	Stability in vitro		Stability in vivo		Ref.
		method	intact complex, %	bone uptake, % of the injected dose per gram (%ID/g)	time point	
BF_4	Trastuzumab			18.9 ± 1.1	96 h	[64]
DFO				2.9 ± 1.0		
BPDET-LysH22,2-3-HOPO	Trastuzumab	Blood serum (4 days)	~40	15.1 ± 2.7	144 h	[67]
DFO				10.6 ± 1.0		
FSC	ZEGFR:2377	1000-fold excess of EDTA (24 h)	85.7 ± 0.4	0.1 ± 0.3	24 h	[79]
DFO			67.7 ± 3.6	1.0 ± 0.3		
p-Bn-NCS-HOPO	Trastuzumab	Blood serum (7 days)	89.2 ± 0.9	2.4 ± 0.3	366 h	[80]
DFO			94.7 ± 0.7	17.0 ± 4.1		
3,2-HOPO	MSLN-mAb	Blood serum (4 days)	23	15.40 ± 2.40	144 h	[81]
DFO	MSLN-mAb		46	6.51 ± 1.82		
YM103	Trastuzumab	Blood serum (7 days)	>95	25.9 ± 0.6	168 h	[82]
DFO			>95	6.5 ± 0.4		
THPN	HPG	Blood plasma (5 days)	96 ± 1	8.4 ± 2.2	144 h	[83]
DFO			97 ± 0	3.3 ± 0.4		
DFO*			>99	3.1 ± 0.7		

DUR was 17.5 ± 5.6 and the tumor/muscle DUR was 21.9 ± 2.2) compared to that of **XI** (tumor/blood DUR of 13.7 ± 2.0; tumor/muscle DUR of 18.6 ± 3.2).

Yet another example of the synthesis of macrocyclic chelators for zirconium was reported in [64]. The authors prepared various hydroxamate-modified macrocyclic chelators L^1–L^3 (Scheme 7). According to the stability challenge results (incubation in 50 mM EDTA), all of the [^{89}Zr]Zr-$L^{1–3}$ complexes were less stable than [^{89}Zr]Zr-DFO. The authors interpreted the lower stability of complexes with the synthesized chelators using quantum chemical calculations: due to steric restrictions, the complex formation of ^{89}Zr with L^1 and L^3 gave seven-coordinate (six-coordinate for L^2) rather than eight-coordinate complexes. Subsequently, after the quantum chemical structure optimization, a new chelator L^4 (Scheme 7) and its bifunctional derivative BF_4 were synthesized. The in vitro stability testing showed approximately equal stabilities for [^{89}Zr]Zr-L^4 (87% intact) and [^{89}Zr]Zr-DFO (91%) in the presence of excess EDTA and a higher stability in blood plasma in the case of [^{89}Zr]Zr-L^4 (94%) compared to [^{89}Zr]Zr-DFO (53%). A comparative in vivo study included two stages: first, the biodistribution of [^{89}Zr]Zr-DFO and [^{89}Zr]Zr-L^4 in the body of healthy mice was estimated. Both complexes showed high renal clearance (>98% of the injected activity was excreted in 30 min). A markedly higher bone tissue uptake for [^{89}Zr]Zr-L^4 (0.60 ± 0.19%ID/g) compared to [^{89}Zr]Zr-DFO (0.05 ± 0.02%ID/g) can be noted. The uptakes in other tissues differed insignificantly. In the second stage, cellular binding assays and comparative studies of [^{89}Zr]Zr-BF_4-trastuzumab and [^{89}Zr]Zr-DFO-trastuzumab biodistribution in mice bearing HER2+ and HER2– tumors were carried out. According to the results, both agents showed equivalent affinity, immunoreactivity, and equal uptakes in all main tissues and organs except for the bone tissue. In the bone tissue, markedly higher uptake was noted for [^{89}Zr]Zr-BF_4-trastuzumab than for [^{89}Zr]Zr-DFO-trastuzumab (Table 4).

Special mention should be made of a study [65] in which the authors carried out preliminary quantum chemical calculations to determine the optimal structure and then synthesized the macrocyclic chelator CTH36 (Scheme 8) containing four hydroxamate groups and tetrazine derivatives tCTH36 and tDFO. Subsequently, these derivatives were conjugated with *trans*-cyclooctene-modified RGDfK analogue (TCO-c(RGDfK)) and used for the synthesis of [^{89}Zr]Zr-CTH36-c(RGDfK) and [^{89}Zr]Zr-DFO-c(RGDfK). The obtained complex based on CTH36

proved to be more stable on incubation in excess EDTA than the similar complex based on DFO. The authors also reported continuation of this study and transition to in vivo stability testing of the complexes.

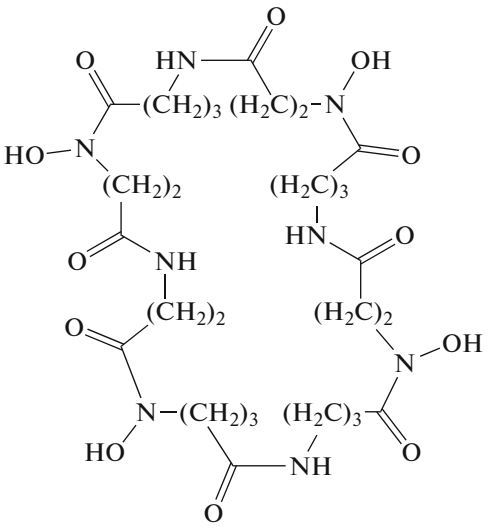

CTH36

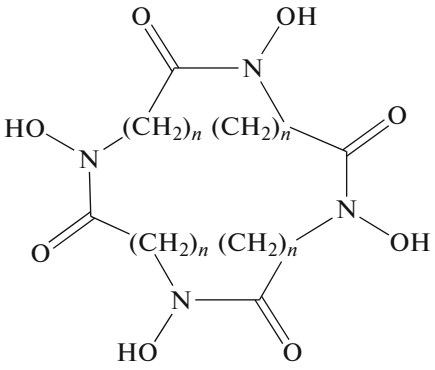

C^5–C^7 (n = 5–7)

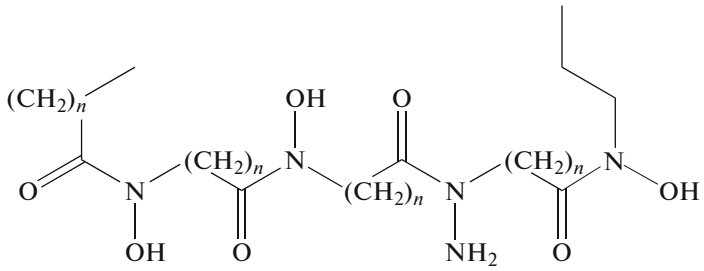

L^5–L^7 (n = 5–7)

Scheme 8.

A comparative study of linear and cyclic hydroxamates was carried out in [78]. The authors synthesized three macrocycles differing in the cavity size (28–36-membered rings) and their acyclic analogues (Scheme 8). All of the synthesized chelators showed lower complexation rates than DFO; the highest radiochemical yield (>99%) was attained for C^7 and L^7 (Scheme 8) after incubation for 120 min at 20°C. The stability of the complexes was determined in a 0.1 M phosphate buffered saline (pH 6.5) an in a 1750-fold excess of EDTA (pH 7). The highest stability was found for the ^{89}Zr complexes with the chelators (>70% of the complex remained intact after 7 days of incubation in the presence of excess EDTA). The ^{89}Zr complexes with C^6, L^6, and DFO noticeably decomposed (less than 50% intact). In the case of ^{89}Zr[Zr]-C^5 and ^{89}Zr[Zr]-L^5, complete transchelation occurred within several minutes. Additionally, complexes with cyclic chelators (n = 5 and 6) were less stable than analogous complexes with their acyclic analogues. The results were in good agreement with the results of quantum mechanical calculations [78].

Thus, the use of cyclic chelators is justified only in the case of optimal relationship between the cavity and cation sizes, since otherwise the arising steric limitation deteriorate the stability of the resulting complexes. In this respect, now it is most appropriate to use acyclic chelators, which most often give more stable complexes in high yields under milder conditions of synthesis.

CHELATORS BASED ON HYDROXYPYRIDONE

Initially, various types of hydroxypyridone (HOPO) derivatives were proposed as efficient chelators to treat the plutonium-238 poisoning [84]. Among the studied chelators, 3,4,3-(LI-1,2-HOPO) and DFO-HOPO proved to be most promising. Further studies of these chelators demonstrated that they are also suitable for chelation of ^{89}Zr. In [66], the hybrid chelator DFO-HOPO was synthesized and studied (Scheme 9). The [^{89}Zr]Zr-DFO-HOPO complex remained stable in blood serum and in EDTA and DFO solutions for 7 days. It was additionally noted that DFO-HOPO can transchelate ^{89}Zr from the DFO complex with high efficiency (>60% in 1 h). A comparative *in vivo* study showed fast clearance and lower bone uptake for [^{89}Zr]Zr-DFO-HOPO compared with [^{89}Zr]Zr-DFO (0.004 ± 0.001 and 0.037 ± 0.002%ID/g 24 h after i/v administration for [^{89}Zr]Zr-DFO-HOPO and [^{89}Zr]Zr-DFO, respectively). Additionally, a markedly higher intestinal uptake was noted for [^{89}Zr]Zr-DFO-HOPO, which was due to high lipophilicity of the complex (Table 2). Despite the highly promising results obtained, the experimental results reported in this paper were obtained for complexes, which have a faster pharmacokinetics than the conjugates prepared from these complexes. For objective estimation of the long-term stability, additional experiments with vectors such as mAbs are required.

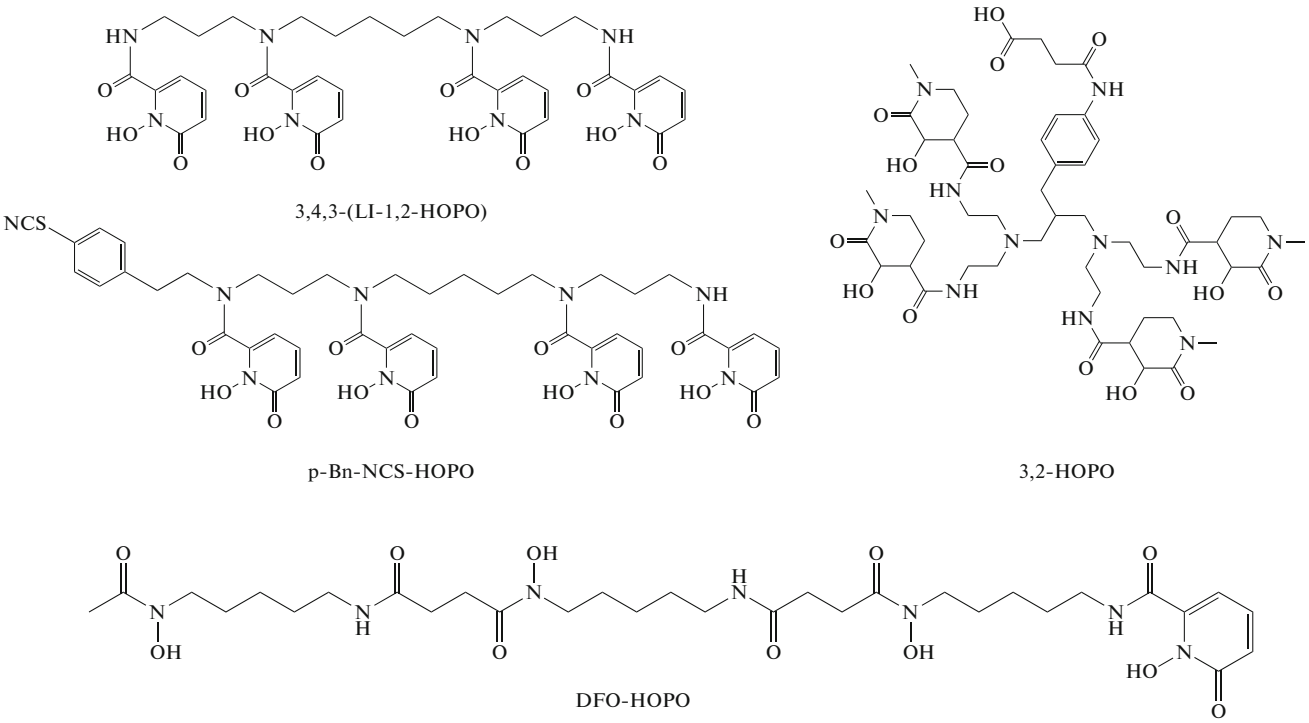

Scheme 9.

The synthesis and detailed study of the chelator (3,4,3-(LI-1,2-HOPO) (Scheme 9) was performed in [85]. The formation of the Zr-HOPO complex in 1 : 1 ratio was confirmed by high-resolution mass spectrometry (HRMS). A comparative study of the complexes showed that [^{89}Zr]Zr-3,4,3-(LI-1,2-HOPO) was stable in blood serum, EDTA solutions (pH 5–8), and DFO solutions for 7 days, whereas a similar complex with DFO underwent considerable transchelation, especially when pH decreased (from 8 to 5). The authors additionally estimated the stability of the complexes in the presence of competing metals (10-fold excess). Under these conditions, both complexes were relatively stable (more than 95% intact) except for the experiment in the presence of Fe^{3+}. The incubation with excess Fe^{3+} resulted in more pronounced substitution for [^{89}Zr]Zr-DFO (39% intact) compared to [^{89}Zr]Zr-HOPO (83% intact). These results are quite expectable, because DFO is a siderophore and has a high affinity to Fe^{3+}. A comparative in vivo study of [^{89}Zr]Zr-HOPO and [^{89}Zr]Zr-DFO showed slower excretion and somewhat higher bone uptake for [^{89}Zr]Zr-3,4,3-(LI-1,2-HOPO) (0.17 ± 0.03%ID/g) in comparison with [^{89}Zr]Zr-DFO (0.06 ± 0.01%ID/g). In the subsequent studies, 3,4,3-(LI-1,2-HOPO) was modified by adding a benzylisothiocyanate group (Scheme 9) and conjugated with trastuzumab [80]. Despite the slight decrease in the in vitro

stability for [^{89}Zr]Zr-HOPO-trastuzumab versus [^{89}Zr]Zr-DFO-trastuzumab (Table 4), in vivo assays showed a lower bone uptake for [^{89}Zr]Zr-HOPO-trastuzumab (Table 4) and a higher tumor/skeleton DUR (~26) compared to analogous sample based on DFO (tumor/skeleton DUR ~8).

Other chelators based on hydroxypyridone showed, unfortunately, less impressive results. Although [^{89}Zr]Zr-BPDET-LysH22,2-3-HOPO (Scheme 10) was more stable against transchelation in DTPA, in vivo studies of this complex and the agent [^{89}Zr]Zr-2,3-HOPO-p-Phe-NCS-trastuzumab derived from this complex showed a higher kidney, liver, and skeletal uptakes than [^{89}Zr]Zr-DFO or [^{89}Zr]Zr-DFO-trastuzumab (Table 4) [67]. These results are in good agreement with another publication [81], in which the authors synthesized radioimmunoconjugates based on 3,2-HOPO (Scheme 9) and DFO with mesothelin-targeting mAb (MSLN-mAb, anrtumab). Estimation of the stability of the obtained agents in blood serum showed lower stability of [^{89}Zr]Zr-3,2-HOPO-MSLN-mAb compared to [^{89}Zr]Zr-DFO-MSLN-mAb (Table 4). The subsequent in vivo study also confirmed a low stability for the agent based on 3,2-HOPO. In the case of [^{89}Zr]Zr-3,2-HOPO-MSLN-mAb, higher and increasing femur uptake was observed (Table 4). Additionally, higher tumor uptake was noted and, hence, higher DURs for the DFO-based material compared to the 3,2-HOPO-based one (tumor uptakes of 28.49 ± 3.78 and 7.97 ± 0.77%ID/g for [^{89}Zr]Zr-DFO-MSLN-mAb and [^{89}Zr]Zr-3,2-HOPO-MSLN-mAb, respectively). Similar results were obtained for the chelators CP256, YM103, and THPN(p-SCN-Bn-THPN) (Scheme 10).

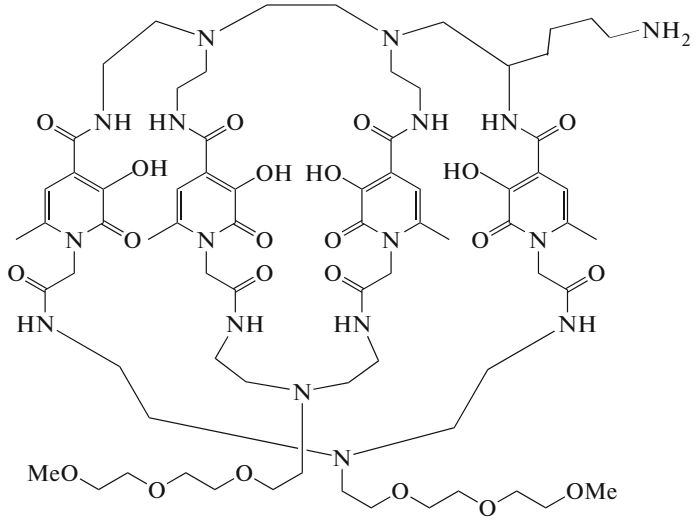

BPDET-LysH22,2-3-HOPO

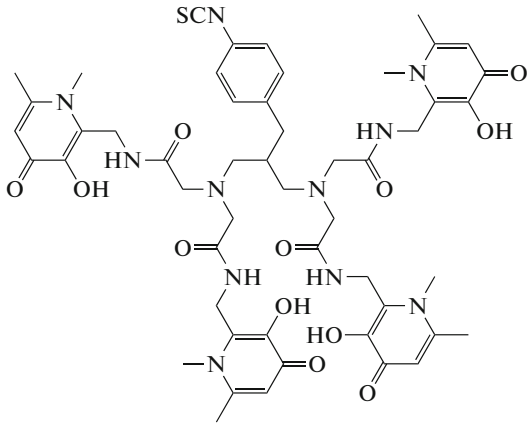

p-SCN-Bn-THPN

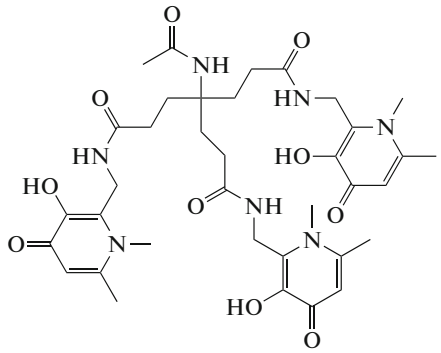

CP256

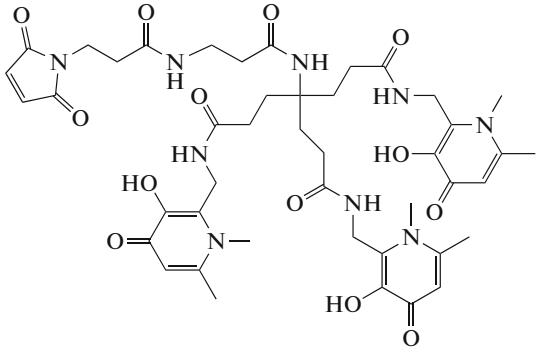

YM103

Scheme 10.

The synthesis of the chelator CP256 and its bifunctional derivative YM103 (Scheme 10) was reported in [82]. The formation of 1 : 1 complex of CP256 with Zr was confirmed by mass spectrometry. A comparative in vitro study of the complexes stability was carried out in the presence of 1, 10, and 100 equivalents of DFO or

CP256 for [^{89}Zr]Zr-CP256 and [^{89}Zr]Zr-DFO, respectively. Under these conditions, [^{89}Zr]Zr-CP256 was more stable than [^{89}Zr]Zr-DFO. The addition of DFO to [^{89}Zr]Zr-CP256 was accompanied by substantial transchelation of [^{89}Zr]Zr-CP256 (in 10- and 100-fold excess of DFO, ~80 and ~15% of the complex, respectively, were intact), whereas the addition of 10- and 100-fold excess of CP256 to [^{89}Zr]Zr-DFO resulted in complete substitution. It is noteworthy that, despite the higher stability in the presence of Fe^{3+} ions (1 mM), the complex [^{89}Zr]Zr-CP256 (CP256 concentration is 0.1 mM) proved to be less stable (~14% intact) than similar DFO complex (~93% intact). Subsequently, the chelators YM103 and p-Bn-NCS-DFO were conjugated with trastuzumab and labeled with ^{89}Zr. Both synthesized agents were prepared with high radiochemical yields (>98%) and remained stable in blood serum for 7 days (Table 4). An in vivo study revealed almost identical biodistributions for [^{89}Zr]Zr-YM103-trastuzumab and [^{89}Zr]Zr-DFO-trastuzumab within 6 h after the injection. However, on further observation, the authors noted a significant increase in the bone tissue uptake for the agent based on YM103 (8.3 ± 0.1%ID/g after 6 h; 25.9 ± 0.6%ID/g after 7 days), but no such trend for the DFO-based sample (7.7 ± 0.7%ID/g after 6 h; 6.5 ± 0.4%ID/g after 7 days).

The results obtained for the chelator THPN were similar (Scheme 10). A comparative in vitro stability study of the complexes [^{89}Zr]Zr-THPN and [^{89}Zr]Zr-DFO showed identical stability for these complexes in blood serum and a higher stability of [^{89}Zr]Zr-THPN in a 100-fold excess of EDTA [68]. An in vivo assay revealed similar biological behaviors for [^{89}Zr]Zr-THPN and [^{89}Zr]Zr-DFO within 24 h after the administration. In the next stage of the study, THPN was conjugated with 1,4-phenylene diisothiocyanate [83]. For the comparative study, p-SCN-Bn-THPN, DFO, and DFO* were conjugated with high-molecular-weight (800 kDa) polymeric hyperbranched polyglycerol (HPG) and labeled with ^{89}Zr. An *in vivo* study on healthy mice revealed the highest bone uptake for [^{89}Zr]Zr-THPN-HPG in comparison with [^{89}Zr]Zr-DFO-HPG and [^{89}Zr]Zr-DFO*-HPG (Table 4). Thus, despite the high thermodynamic stability of the [^{89}Zr]Zr-THPN complex (logβ = 50.3) and higher in vitro stability compared to that of [^{89}Zr]Zr-DFO, the THPN-based agent was less stable when studied in vivo and had a higher bone uptake. Among the possible causes for the unsatisfactory stability, the introduction of the *p*-phenylene diisothiocyanate group was indicated, since, according to quantum chemical calculations, this leads to a slight disruption of the coordination geometry.

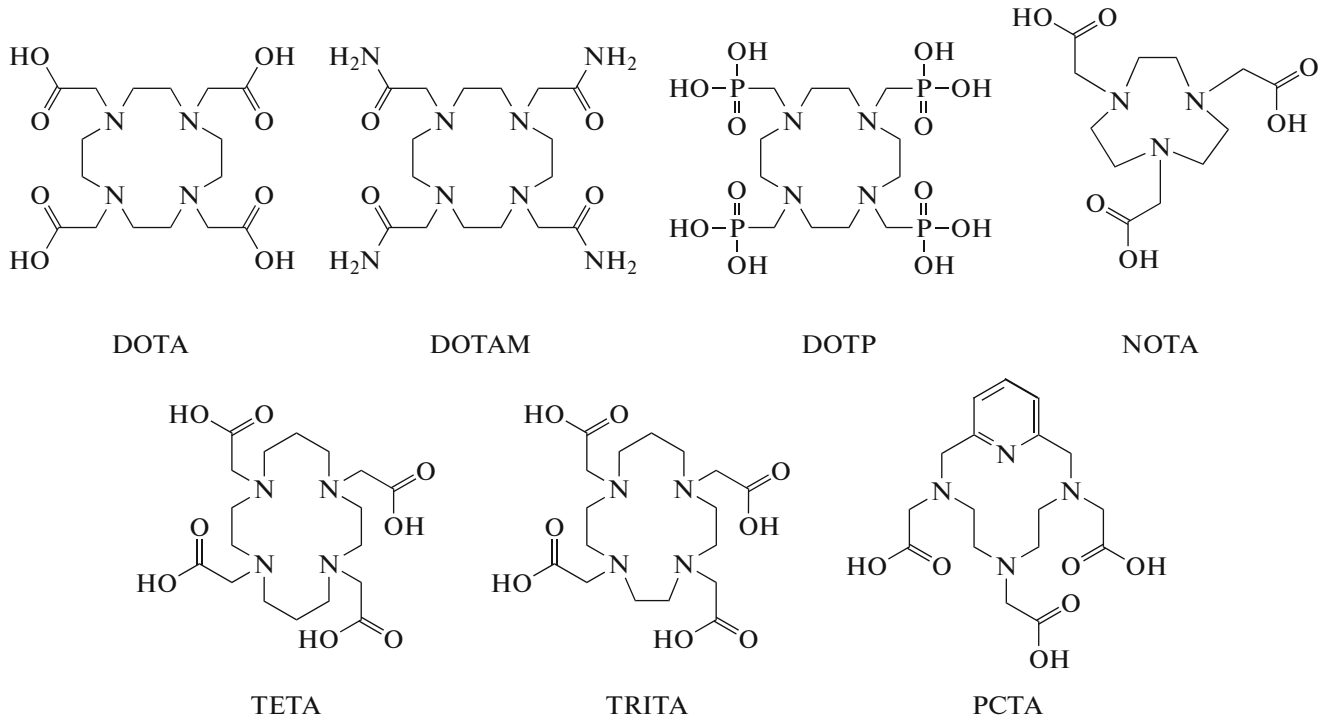

Scheme 11.

MISCELLANEOUS CHELATORS

The ^{89}Zr complexes with chelators DOTA, DOTAM, DOTP, NOTA, TETA, TRITA, and PCTA (Scheme 11) [71, 72] and with new chelators containing four hydroxyisophthalimide (IAM-1 and IAM-2) [69] or dihydroxyterephthalamide (TAM-1 and TAM-2) groups [70] were studied.

While considering these chelators, it is important to take into account the possibility of conducting the reaction without additional heating (Table 2). In this context, only the [^{89}Zr]Zr-TAM-1 and [^{89}Zr]Zr-TAM-2 complexes (Scheme 12) can be obtained under the same conditions as [^{89}Zr]Zr-DFO.

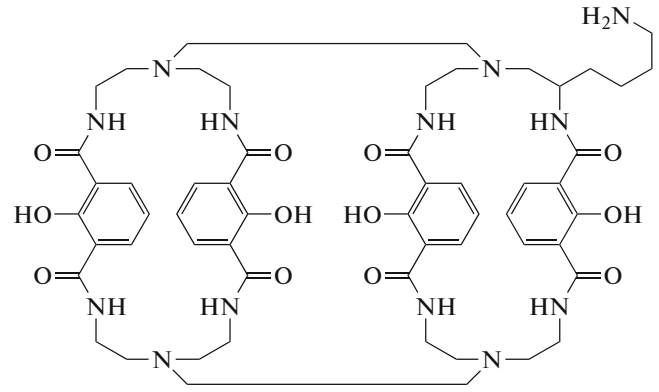

IAM-1

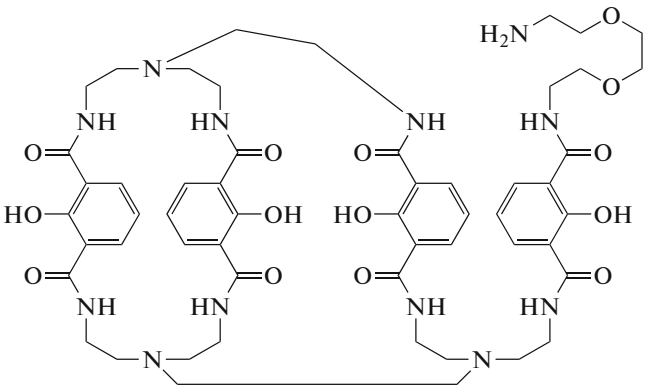

IAM-2

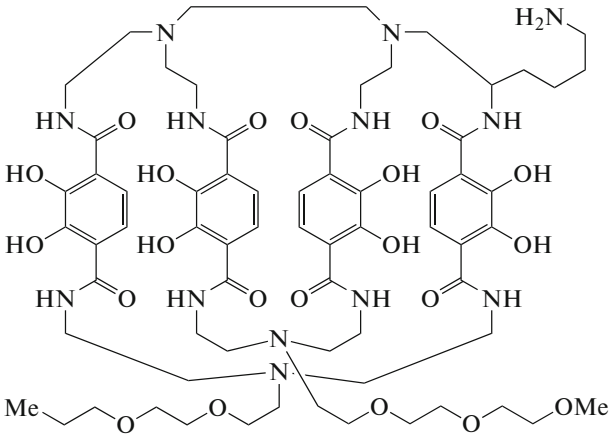

TAM-1

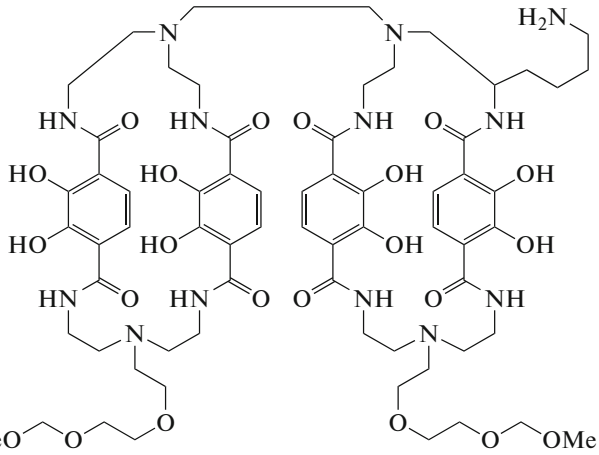

TAM-2

Scheme 12.

Stability assays in vitro for [^{89}Zr]Zr-IAM-1 and [^{89}Zr]Zr-IAM-2 showed that [^{89}Zr]Zr-IAM-1 was more stable (72% intact) in the presence of excess DTPA (50 mM, incubation for 7 days) than [^{89}Zr]Zr-DFO (41% intact) or [^{89}Zr]Zr-IAM-2 (26% intact) [69]. However, incubation in a blood serum gave opposite results: [^{89}Zr]Zr-DFO was stable, whereas for [^{89}Zr]Zr-IAM-1 and [^{89}Zr]Zr-IAM-2, only 75 and 17% of the initial complex remained intact, respectively. The subsequent in vivo assays confirmed the lower stability of the prepared complexes. The [^{89}Zr]Zr-IAM-1 and [^{89}Zr]Zr-IAM-2 complexes showed markedly higher liver and bone uptakes (the bone uptakes 72 h after the administration were 0.08 ± 0.01%ID/g for [^{89}Zr]Zr-DFO; 0.11 ± 0.01%ID/g for [^{89}Zr]Zr-IAM-1; and 0.68 ± 0.33%ID/g for [^{89}Zr]Zr-IAM-2). Different uptake dynamics in the bone tissue can be noted for [^{89}Zr]Zr-IAM-1 and [^{89}Zr]Zr-IAM-2: in the case of [^{89}Zr]Zr-IAM-1, the uptake gradually decreased, which may be attributable to perfusion and low clearance, whereas in the case of [^{89}Zr]Zr-IAM-2, the uptake increased, which was due to the lower stability of this complex. The stability difference between [^{89}Zr]Zr-IAM-1 and [^{89}Zr]Zr-IAM-2 may be caused by the less rigid structure of the chelator IAM-2, which forms more labile complexes with ^{89}Zr.

Similar results were obtained with chelators TAM-1 and TAM-2 [70]. In the presence of excess DTPA (50 mM, incubation for 7 days at 37°C), the [^{89}Zr]Zr-TAM-1 and [^{89}Zr]Zr-TAM-2 complexes were more stable (100% intact) than [^{89}Zr]Zr-DFO (41% intact). Studies of [^{89}Zr]Zr-TAM-1 and [^{89}Zr]Zr-TAM-2 in vivo revealed a higher stability and a higher clearance for [^{89}Zr]Zr-TAM-1. A comparative study of [^{89}Zr]Zr-TAM-1 and [^{89}Zr]Zr-DFO noted an insignificant difference in the bone uptakes (0.078 ± 0.014%ID/g for [^{89}Zr]Zr-DFO; and 0.074 ± 0.022%ID/g for [^{89}Zr]Zr-TAM-1) and a higher liver and kidney uptakes. Thus, despite the higher stability *in vitro*, the obtained complexes do not possess a sufficient kinetic stability.

It should be noted that since zirconium-89 is mainly used to obtain agents based on monoclonal antibodies using DFO as a chelator, the complex formation and stability for azamacrocyclic chelators have not been studied in detail. Rather recently, a detailed study of ^{89}Zr complexation with DOTA, DOTP, and DOTAM was reported [71]. According to the presented data, ^{89}Zr forms very stable complexes with DOTA (Scheme 11). The stability of ^{89}Zr complexes with DOTA, DOTP, and DOTAM decreases in the following order: [^{89}Zr]Zr-DOTA ≫ [^{89}Zr]Zr-DOTP > [^{89}Zr]Zr-DOTAM > [^{89}Zr]Zr-DFO. The authors noted that [^{89}Zr]Zr-DOTA is not transchelated even in the presence of a 1000-fold excess of EDTA within 7 days. Under similar conditions, only 20% of ^{89}Zr is retained in the [^{89}Zr]Zr-DFO complex. The subsequent comparative in vivo study demonstrated that, among the tested complexes, the lowest non-specific uptake (blood, bones, liver, kidneys) is inherent in [^{89}Zr]Zr-DOTA. However, it should be borne in mind that the possibility of using DOTA for the synthesis of ^{89}Zr-RPs is significantly limited: the formation of [^{89}Zr]Zr-DOTA requires heating (>70°C for 30 min or more), which precludes the use of preconjugated antibodies. Moreover, even if the concept of prelabeling and subsequent conjugation is implemented, the scope of DOTA applicability as a chelator is significantly limited. The [^{89}Zr]Zr-DOTA complex cannot be conjugated with a vector molecule, since it has no free carboxyl groups.

Later, the authors published one more detailed study of chelators TETA, TRITA, PCTA, and NOTA (Scheme 11) [72]. The Zr-TRITA, Zr-PCTA, and Zr-NOTA complexes were obtained in high yields and characterized by various methods (HPLC, NMR, HRMS). The authors also presented the results of X-ray diffraction studies of the obtained compounds, which indicated the formation of binuclear complexes, $[Zr(PCTA)]_2O{\cdot}8H_2O$ and $[Zr(NOTA)(OH)]_2{\cdot}6H_2O$, due to insufficient denticity of the chelators. The [^{89}Zr]Zr-PCTA, [^{89}Zr]Zr-NOTA, and [^{89}Zr]Zr-TRITA complexes formed in quantitative yields (Table 2). The complex with TETA could not be synthesized. For estimating the stability, the resulting complexes were incubated in the presence of excess metal salts or EDTA and in blood serum. The highest stability against transchelation in the presence of a 1000-fold excess of EDTA (pH 5–7) was found for [^{89}Zr]Zr-PCTA (100% intact after 7 days of incubation at 37°C), while [^{89}Zr]Zr-NOTA was markedly transchelated (70.7% intact), and [^{89}Zr]Zr-TRITA completely dissociated (9.6% intact). Similar results were obtained on incubation in blood serum and in the presence of metal salts. It is also noteworthy that despite the introduction of the pyridine ring into the PCTA molecule, [^{89}Zr]Zr-PCTA is more hydrophilic than [^{89}Zr]Zr-NOTA and [^{89}Zr]Zr-DFO (Table 2). A comparative in vivo study of the complexes showed a lower clearance for [^{89}Zr]Zr-TRITA and correspondingly higher uptakes in all organs and tissues. Moreover, after 48 h, bone tissue uptake was found to increase fourfold, which confirmed the unsatisfactory stability of [^{89}Zr]Zr-TRITA. Generally, the biodistribution of [^{89}Zr]Zr-PCTA and [^{89}Zr]Zr-NOTA was similar to that of [^{89}Zr]Zr-DFO: the complexes had low clearance and correspondingly high non-specific uptake compared to the above-presented results for [^{89}Zr]Zr-DOTA.

To summarize, mention should be made of a recent study [86], devoted to the direct comparison of chelators of different groups: DFO*, CTH36, 3,4,3-(LI-1,2-HOPO), and DOTA-GA. The authors synthesized tetrazine-modified chelators, which were subsequently conjugated with the peptide, c(RGDfK), and labeled with ^{89}Zr. The ^{89}Zr complexes with DFO-c(RGDfK), DFO*-c(RGDfK), and CTH36-c(RGDfK) were obtained in high yields (>96%) after 1 h of incubation at 37°C; the synthesis of [^{89}Zr]Zr-3,4,3-(LI-1,2-HOPO)-c(RGDfK) required heating for 5 h and gave several forms of complexes. The complex with DOTA-GA-c(RGDfK) could not be synthesized even by incubation at 99°C for several hours. The authors noted that, according to quantum chemical calculations, modification of the chelator molecule with tetrazine had little effect on the molecular geometry, except for the complex with DOTA-GA, in which the Zr–N bonds were elongated compared to those in Zr-DOTA. Nevertheless, this fact does not explain the zero yield of the complexation reaction. For estimating the stability, the obtained complexes were incubated in a 10000-fold excess of EDTA for 54 h. Under these conditions, the [^{89}Zr]Zr-DFO-c(RGDfK) complex rapidly dissociated (<10% of the complex was intact after 24 h). The complexes [^{89}Zr]Zr-DFO*-c(RGDfK) and [^{89}Zr]Zr-3,4,3-(LI-1,2-HOPO)-c(RGDfK) were sufficiently stable throughout the experiment (>80 and >95% intact, respectively). Of most interest is the fact that the complex based on the chelator CTH36 was somewhat more stable than

[^{89}Zr]Zr-DFO-c(RGDfK) (~10% of the complex was intact after 24 h). According to quantum chemical calculations (B3LYP, DGDZVP basis set), CTH36 forms a Zr complex characterized by one of the highest thermodynamic stability constants (Table 5) [32]. In addition to CTH36 ^{89}Zr stable complexes with oxoDFO*, DFO-HOPO, DFO*, CTH36, and THPN are formed (Table 5).

The higher thermodynamic stability of Zr(oxoDFO*) is, in this case, attributable to higher flexibility of the oxoDFO* structure caused by the presence of ether bridges in the chelator molecule, which decrease the steric hindrance. This effect can also be observed while comparing the $[ZrDFO(H_2O)]^+$ and $[Zr(DFO\text{-}O3)]^+$ complexes (Table 5). Thus, the introduction of ether bridges is probably one of the most successful approaches to modification of chelators, because it simultaneously increases both the thermodynamic stability and hydrophilicity of the initial molecule. Apart from CTH36 and DFO derivatives, high thermodynamic stability constant is also inherent in the Zr complex with THPN; however, in practice, THPN-based agents are less stable *in vivo* than similar agents based on DFO and DFO* [83]. These results confirm once again that thermodynamic constants are useful for the preliminary comparisons of different chelators, but cannot be used to evaluate the in vivo stability of the complexes.

In conclusion, it should be noted that a considerable progress has been attained in the ^{89}Zr radiopharmaceutical chemistry in the last decade. Currently, various zirconium-89 pharmaceuticals are being introduced in the clinical practice. Despite the promising results of clinical and preclinical trials of new ^{89}Zr-RPs, the agents based on the chelator deferoxamine are prone to dissociation in vivo. This gave an impetus for the development and detailed investigation of quite a few novel chelators for ^{89}Zr. The main challenge in the design of a new "ideal" chelator is the pronounced difference between the thermodynamic and kinetic stabilities of the obtained complexes. Consequently, despite the high stability of most new chelators in vitro, the obtained complexes, like the complex with DFO, dissociated in vivo. In addition, a requirement to the chelator is the possibility of fast conjugation with a vector molecule and conduction of the complex formation without additional heating. Currently, considering the sum of published results, DFO*, which proved to be effective in a number of studies, can be taken as the most promising chelator, together with the derivative oxoDFO*, which is more hydrophilic and, according to preliminary estimates, forms more stable complexes with ^{89}Zr than DFO*.

To date, more than 30 clinical trials with ^{89}Zr have been planned or are in progress, and more than 20 trials have been completed [87]. Most of the described zirconium-89 RPs are based on monoclonal antibodies (an example is [^{89}Zr]Zr-trastuzumab widely used for breast cancer diagnosis). Unfortunately, in Russia, zirconium-89-based agents are at an early stage of development and are not yet routinely used in medical facilities. The main complications in this case are both the absence of well-developed manufacture of ^{89}Zr, which restricts further studies by various research groups, and the absence of clear legal regulations for the clinical use of unregistered new RPs. Since the application of RPs has become an integral part of high-quality and high-tech medical care in developed countries, there is every reason to believe that these difficulties will be overcome in the near future.

Table 5. Thermodynamic stability constants for some complexes [32]

Complex	logβ
Zr(oxoDFO*)	54.16
Zr(DFO-HOPO)	53.51
Zr(DFO*)	51.56
Zr(CTH36)	52.84
Zr(THPN)	47.28
$[ZrDFO(H_2O)]^+$	41.41
$[Zr(DFO\text{-}O3)]^+$	43.37

CONFLICT OF INTEREST

The authors declare that they have no conflicts of interest.

REFERENCES

1. van Dongen, G.A.M.S., Beaino, W., Windhorst, A.D., et al., *J. Nucl. Med.*, 2021, vol. 62, no. 4, p. 438.
2. Mendler, C.T., Gehring, T., Wester, H.-J., et al., *J. Nucl. Med.*, 2015, vol. 56, no. 7, p. 1112.
3. Cheal, S.M., Punzalan, B., Doran, M.G., et al., *Eur. J. Nucl. Med. Mol. Imaging*, 2014, vol. 41, no. 5, p. 985.
4. Berg, E., Gill, H., Marik, J., et al., *J. Nucl. Med.*, 2020, vol. 61, no. 3, p. 453.
5. Disselhorst, J.A., Brom, M., Laverman, P., et al., *J. Nucl. Med.*, 2010, vol. 51, no. 4, p. 610.
6. Conti, M. and Eriksson, L., *EJNMMI Phys.*, 2016, vol. 3, no. 1.
7. Sánchez-Crespo, A., Andreo, P., and Larsson, S.A., *Eur. J. Nucl. Med. Mol. Imaging*, 2004, vol. 31, no. 1, p. 44.
8. Marquez-Nostra, B.V. and Viola, N., in *Radiopharmaceutical Chemistry*, Lewis, J.S., Windhorst, A.D., and Zeglis, B.M., Eds., Springer Cham, 2019, p. 371.
9. McKnight, B.N. and Viola-Villegas, N.T., *J. Label. Compd. Radiopharm.*, 2018, vol. 61, no. 9, p. 727.
10. Yoon, J.-K., Park, B.-N., Ryu, E.-K., et al., *Int. J. Mol. Sci.*, 2020, vol. 21, no. 12, p. 4309.

11. Kurebayashi, Y., Choyke, P.L., and Sato, N., *Nanotheranostics*, 2021, vol. 5, no. 1, p. 27.
12. De Feo, M.S., Pontico, M., Frantellizzi, V., et al., *Clin. Transl. Imaging*, 2022, vol. 10, no. 1, p. 23.
13. Laboratoire National Henri Becquerel. http://www.lnhb.fr/en/.
14. Link, J.M., Krohn, K.A., and O'Hara, M.J., *Appl. Radiat. Isot.*, 2017, vol. 122, p. 211.
15. Queern, S.L., Aweda, T.A., Massicano, A.V.F., et al., *Nucl. Med. Biol.*, 2017, vol. 50, p. 11.
16. Alnahwi, A.H., Tremblay, S., and Guérin, B., *Appl. Sci.*, 2018, vol. 8, no. 9, p. 1.
17. Meijs, W.E., Herscheid, J.D.M., Haisma, H.J., et al., *Appl. Radiat. Isot.*, 1994, vol. 45, no. 12, p. 1143.
18. Verel, I., Visser, G.W.M., Boellaard, R., et al., *J. Nucl. Med.*, 2003, vol. 44, no. 8, p. 1271.
19. Holland, J.P., Sheh, Y., and Lewis, J.S., *Nucl. Med. Biol.*, 2009, vol. 36, no. 7, p. 729.
20. Graves, S.A., Kutyreff, C., Barrett, K.E., et al., *Nucl. Med. Biol.*, 2018, vols. 64–65, p. 1.
21. Pandya, D.N., Bhatt, N.B., Almaguel, F., et al., *J. Nucl. Med.*, 2019, vol. 60, no. 5, p. 696.
22. Bubenshchikov, V.B., Larenkov, A.A., and Kodina, G.E., *Radiochemistry*, 2021, vol. 63, no. 3, p. 369.
23. Intorre, B.J. and Martell, A.E., *J. Am. Chem. Soc.*, 1961, vol. 83, no. 17, p. 3618.
24. Intorre, B.I. and Martell, A.E., *J. Am. Chem. Soc.*, 1960, vol. 82, no. 2, p. 358.
25. Shannon, R.D., *Acta Crystallogr., Sect. A: Cryst. Phys., Diffr., Theor. Gen. Crystallogr.*, 1976, vol. 32, no. 5, p. 751.
26. Pozhidaev, A.I., Porai-Koshits, M.A., and Polynova, T.N., *J. Struct. Chem.*, 1974, vol. 15, no. 4, p. 548.
27. Ilyukhin, A.B., Davidovich, R.L., Samsonova, I.N., et al., *Cryst. Rep.*, 2000, vol. 45, no. 1, p. 39.
28. Friend, M.T. and Wall, N.A., *Inorg. Chim. Acta*, 2019, vol. 484, p. 357.
29. Meijs, W.E., Herscheid, J.D.M., Haisma, H.J., et al., *Int. J. Radiat. Appl. Inst. A*, 1992, vol. 43, no. 12, p. 1443.
30. Bickel, H., Gäumann, E., Keller-Schierlein, W., et al., *Experientia*, 1960, vol. 16, no. 4, p. 129.
31. Holland, J.P., Divilov, V., Bander, N.H., et al., *J. Nucl. Med.*, 2010, vol. 51, no. 8, p. 1293.
32. Holland, J.P., *Inorg. Chem.*, 2020, vol. 59, no. 3, p. 2070.
33. Racow, E.E., Kreinbihl, J.J., Cosby, A.G., et al., *J. Am. Chem. Soc.*, 2019, vol. 141, no. 37, p. 14650.
34. Summers, K.L., Sarbisheh, E.K., Zimmerling, A., et al., *Inorg. Chem.*, 2020, vol. 59, no. 23, p. 17443.
35. Ekberg, C., Källvenius, G., Albinsson, Y., et al., *J. Solution Chem.*, 2004, vol. 33, no. 1, p. 47.
36. Toporivska, Y. and Gumienna-Kontecka, E., *J. Inorg. Biochem.*, 2019, vol. 198, p. 110753.
37. Savastano, M., Bazzicalupi, C., Ferraro, G., et al., *Molecules*, 2019, vol. 24, no. 11, p. 2098.
38. Imura, R., Ida, H., Sasaki, I., et al., *Molecules*, 2021, vol. 26, no. 16, p. 4977.
39. Price, E.W. and Orvig, C., *Chem. Soc. Rev.*, 2014, vol. 43, no. 1, p. 260.
40. Mealey, J., *Nature*, 1957, vol. 179, no. 4561, p. 673.
41. Zhong, W., Parkinson, J.A., Guo, M., et al., *JBIC J. Biol. Inorg. Chem.*, 2002, vol. 7, no. 6, p. 589.
42. Deri, M.A., Zeglis, B.M., Francesconi, L.C., et al., *Nucl. Med. Biol.*, 2013, vol. 40, no. 1, p. 3.
43. Bhatt, N., Pandya, D., and Wadas, T., *Molecules*, 2018, vol. 23, no. 3, p. 638.
44. Vosjan, M.J.W.D., Perk, L.R., Visser, G.W.M., et al., *Nat. Protoc.*, 2010, vol. 5, no. 4, p. 739.
45. Perk, L.R., Vosjan, M.J.W.D., Visser, G.W.M., et al., *Eur. J. Nucl. Med. Mol. Imaging*, 2010, vol. 37, no. 2, p. 250.
46. Viola-Villegas, N.T., Rice, S.L., Carlin, S., et al., *J. Nucl. Med.*, 2013, vol. 54, no. 11, p. 1876.
47. Perk, L.R., Visser, G.W.M., Vosjan, M.J.W.D., et al., *J. Nucl. Med.*, 2005, vol. 46, no. 11, p. 1898.
48. Oude Munnink, T.H., Korte, M.A. de, Nagengast, W.B., et al., *Eur. J. Cancer*, 2010, vol. 46, no. 3, p. 678.
49. Nayak, T.K., Garmestani, K., Milenic, D.E., et al., *J. Nucl. Med.*, 2012, vol. 53, no. 1, p. 113.
50. Meijs, W.E., Haisma, H.J., Klok, R.P., et al., *J. Nucl. Med.*, 1997, vol. 38, no. 1, p. 112.
51. Abou, D.S., Ku, T., and Smith-Jones, P.M., *Nucl. Med. Biol.*, 2011, vol. 38, no. 5, p. 675.
52. Patra, M., Bauman, A., Mari, C., et al., *Chem. Commun.*, 2014, vol. 50, no. 78, p. 11523.
53. Vugts, D.J., Klaver, C., Sewing, C., et al., *Eur. J. Nucl. Med. Mol. Imaging*, 2017, vol. 44, no. 2, p. 286.
54. Cho, H., Al-saden, N., Lam, H., et al., *Nucl. Med. Biol.*, 2020, vols. 84–85, p. 11.
55. Raavé, R., Sandker, G., Adumeau, P., et al., *Eur. J. Nucl. Med. Mol. Imaging*, 2020, vol. 47, no. 2, p. 505.
56. Adams, C.J., Wilson, J.J., and Boros, E., *Mol. Pharm.*, 2017, vol. 14, no. 8, p. 2831.
57. Rousseau, J., Zhang, Z., Dias, G.M., et al., *Bioorg. Med. Chem. Lett.*, 2017, vol. 27, no. 4, p. 708.
58. Chomet, M., Schreurs, M., Bolijn, M.J., et al., *Eur. J. Nucl. Med. Mol. Imaging*, 2021, vol. 48, no. 3, p. 694.
59. Al-Saden, N., Lam, K., Chan, C., et al., *Mol. Pharm.*, 2018, vol. 15, no. 8, p. 3383.
60. Briand, M., Aulsebrook, M.L., Mindt, T.L., et al., *Dalton Trans.*, 2017, vol. 46, no. 47, p. 16387.
61. Alnahwi, A.H., Ait-Mohand, S., Dumulon-Perreault, V., et al., *ACS Omega*, 2020, vol. 5, no. 19, p. 10731.
62. Zhai, C., Summer, D., Rangger, C., et al., *Mol. Pharm.*, 2015, vol. 12, no. 6, p. 2142.
63. Zhai, C., He, S., Ye, Y., et al., *Biomolecules*, 2019, vol. 9, no. 3, p. 91.
64. Boros, E., Holland, J.P., Kenton, N., et al., *Chempluschem*, 2016, vol. 81, no. 3, p. 274.
65. Seibold, U., Wängler, B., and Wängler, C., *ChemMedChem.*, 2017, vol. 12, no. 18, p. 1555.
66. Allott, L., Da Pieve, C., Meyers, J., et al., *Chem. Commun.*, 2017, vol. 53, no. 61, p. 8529.

67. Tinianow, J.N., Pandya, D.N., Pailloux, S.L., et al., *Theranostics*, 2016, vol. 6, no. 4, p. 511.
68. Buchwalder, C., Rodríguez-Rodríguez, C., Schaffer, P., et al., *Dalton Trans.*, 2017, vol. 46, no. 29, p. 9654.
69. Bhatt, N.B., Pandya, D.N., Xu, J., et al., *PLoS One*, 2017, vol. 12, no. 6, p. e0178767.
70. Pandya, D.N., Pailloux, S., Tatum, D., et al., *Chem. Commun.*, 2015, vol. 51, no. 12, p. 2301.
71. Pandya, D.N., Bhatt, N., Yuan, H., et al., *Chem. Sci.*, 2017, vol. 8, no. 3, p. 2309.
72. Pandya, D.N., Henry, K.E., Day, C.S., et al., *Inorg. Chem.*, 2020, vol. 59, no. 23, p. 17473.
73. Richardson-Sanchez, T., Tieu, W., Gotsbacher, M.P., et al., *Org. Biomol. Chem.*, 2017, vol. 15, no. 27, p. 5719.
74. Brown, C.J.M., Gotsbacher, M.P., and Codd, R., *Aust. J. Chem.*, 2020, vol. 73, no. 10, p. 969.
75. Brandt, M., Cowell, J., Aulsebrook, M.L., et al., *JBIC J. Biol. Inorg. Chem.*, 2020, vol. 25, no. 5, p. 789.
76. Rudd, S.E., Roselt, P., Cullinane, C., et al., *Chem. Commun.*, 2016, vol. 52, no. 80, p. 11889.
77. Liapis, V., Tieu, W., Rudd, S.E., et al., *EJNMMI Radiopharm. Chem.*, 2020, vol. 5, no. 1, p. 27.
78. Guérard, F., Lee, Y.-S., and Brechbiel, M.W., *Chem. A Eur. J.*, 2014, vol. 20, no. 19, p. 5584.
79. Summer, D., Garousi, J., Oroujeni, M., et al., *Mol. Pharm.*, 2018, vol. 15, no. 1, p. 175.
80. Deri, M.A., Ponnala, S., Kozlowski, P., et al., *Bioconjug. Chem.*, 2015, vol. 26, no. 12, p. 2579.
81. Roy, J., Jagoda, E.M., Basuli, F., et al., *Cancer Biother. Radiopharm.*, 2021, vol. 36, no. 4, p. 316.
82. Ma, M.T., Meszaros, L.K., Paterson, B.M., et al., *Dalton Trans.*, 2015, vol. 44, no. 11, p. 4884.
83. Buchwalder, C., Jaraquemada-Peláez, M.D.G., Rousseau, J., et al., *Inorg. Chem.*, 2019, vol. 58, no. 21, p. 14667.
84. White, D.L., Durbin, P.W., Jeung, N., et al., *J. Med. Chem.*, 1988, vol. 31, no. 1, p. 11.
85. Deri, M.A., Ponnala, S., Zeglis, B.M., et al., *J. Med. Chem.*, 2014, vol. 57, no. 11, p. 4849.
86. Damerow, H., Hubner, R., Judmann, B., et al., *Cancers* (Basel), 2021, vol. 13, no. 24, p. 6349.
87. Clinical Trials.gov. http://www.clinicaltrials.gov.

Translated by Z. Svitanko